The Potential use of Tobacco Waste for the Passive Treatment of Acid Mine Drainage

MSc Environmental Engineering Research Report

Prepared by

Hamlton Dovorogwa

Student number: 982722

Submitted to

School of Civil and Environmental Engineering, Faculty of Engineering and the Built Environment, University of the Witwatersrand, Johannesburg, South Africa

Supervisor: Professor Kevin Harding

August 2020

DECLARATION

I declare that this report is my own unaided work, unless otherwise stated. It is being submitted for the award of a degree in Master of Environmental Engineering at the University of the Witwatersrand, Johannesburg. It has not been submitted before for any degree or examination to any other University.

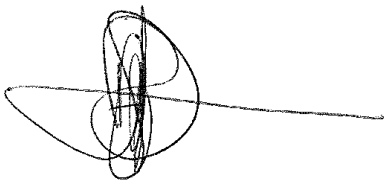

Hamlton Dovorogwa

15 day of **August** year **2020**

Abstract

Tobacco waste (dust and stem) was successfully used as a metal cation adsorbent, pH modifier and carbon/energy source for sulfate reducing bacteria during acid mine drainage (AMD) biotreatment. Firstly, the compositional analysis for both tobacco waste and the AMD were conducted. Batch adsorption and bioremediation tests were then run using the synthetic and gold mining tailing dump-based AMD wastewater. The industrial AMD assayed in (Fe^{2+}-420.23), (Ni^{2+}- 20.32), (Cu^{2+}-38.21), (Zn^{2+}-5.73) and ($SO4^{2}$-3318.23) all in mg/L. Adsorption tests lasted 15 hours, while bioremediation incubation periods were 50 days. For the bioremediation, sulfate reducing bacteria were inoculated into the AMD effluent after growing for some time in a nutrient enriched growth media. Different adsorbent loadings of 20-, 40-, 80- and 160 g/L were tested for adsorption and while 80 g/L was chosen for bioremediation trials. Tobacco waste performance as metal cation adsorbent, AMD pH modifier and energy source for SRBs was monitored by recording metals removal efficiencies, sulfate reduction, pH trends and dissolved COD in the AMD effluent during the trials. Metal removals during adsorption were found to be at maximum of 38-, 41-, 31- and 43% for iron, nickel, copper and zinc respectively. These results were for 80 g/L adsorbent (tobacco waste) loadings. At different loadings, the overall metal removals were lowest for the lowest adsorbent loading of 20 g/L and highest for the highest loading of 160 g/L. The increase in metal removals as adsorbent loading increase were significant between 20 g/L and 80 g/L, and increasing the adsorbent loading further to 160 g/L did not introduce a proportional increase in metal removals, hence no further increases in adsorbent loading were investigated. The Langmuir adsorption isotherm best fitted the iron data while the Sips adsorption isotherm described well the adsorption of nickel, copper and zinc onto tobacco waste. Introducing SRBs in the bioremediation scheme increased the metals removal as well as the sulfate reduction into sulfides and sulfur. The pH of the AMD also increased and a few carbonates and hydroxides also precipitated out. Maximum metal removals in SRB mediated remediation were 95-, 97-, 70- and 93% for iron, nickel, copper and zinc respectively. Copper demonstrated the highest recalcitrance to both adsorption and bioremediation. Sulfate removal reached 63% in synthetic AMD while it was slightly higher at 67% in industrial AMD. The final

AMD pH after the SRB mediated bioremediation went up by 2.05 units starting from a value of 2.7 (industrial) and 3 (synthetic). The metals and sulfate concentration remaining in AMD during AMD treatment can be modelled using the exponential decay function. Overall, the tobacco waste proved to have a high potential both as adsorbent and as carbon source for sulfate reducing bacteria that facilitate AMD biological treatment.

Acknowledgements

Firstly, I would like to thank my Supervisor Professor Kevin Harding for his guidance throughout the research. May I also acknowledge the invaluable support I got from Khatu, my Laboratory Supervisor. Thank you very much and this report is a testimony of your assistance. The Almighty God was in control throughout my studies and it is by his grace that I managed to finish these studies. Thank you Lord.

To my wife Brandina and our three children, Apaishe, Akudzweishe and Arikoishe, thank you for your unwavering moral support and patience throughout my studies. If it was not for the encouragement from you my wife, I would have quitted halfway through. I know it was difficult for you to attend some family functions without me, the missed soccer tournaments and gymnastic festivals. To my twin brother Delford, you have been a pillar of support throughout my academic life. We have traversed together the academic journey since the beginning, and thus far the Lord has taken us.

Table of Contents

DECLARATION i

Abstract ii

Acknowledgements iv

List of Figures ix

List of Tables x

List of Abbreviations, Symbols and Acronyms xi

CHAPTER 1: INTRODUCTION 1

1.1 Background 1

1.2 Sulfate reducing bacteria in AMD treatment 2

1.3 Carbon sources for SRBs 2

1.4 Problem statement 2

1.5 Hypothesis 3

1.7 Research questions 3

1.8 Aim and objectives 3

1.9 Outline of the dissertation 3

CHAPTER 2: LITERATURE REVIEW 5

2.1 Overview 5

2.2 Acid mine drainage formation 5

2.3 AMD challenges 8

2.4 Management of acid mine drainage 8

2.4.1 Treating AMD through passive systems employing SRB 9

2.4.2 Carbon sources for SRB in treating AMD 10

2.4.3 Tobacco waste as carbon source for SRB in AMD treatment 12

2.5 History and economic importance of tobacco processing 13

2.5.1 Challenges from the tobacco industry 13
2.6 Tobacco leaf chemistry and waste potential as SRB substrate 15
CHAPTER 3: EXPERIMENTAL METHODS 17
3.1 Overview 17
3.2 Materials and Chemicals 17
3.2.1 Chemicals 17
3.2.2 Tobacco waste 17
3.2.3 Synthetic AMD 17
3.2.4 Industrial AMD 18
3.2.5 Sulfate reducing bacteria and growth media. 18
3.3 Methods 19
3.3.1 Experimental set-up 19
3.2.2 Tobacco waste characterisation 20
3.2.3 Metal cation measurements 21
3.2.4 COD measurements 21
3.2.5 pH measurements 21
3.2.6 Sulfate concentration measurements 21
3.3 Results Analysis 22
CHAPTER 4: RESULTS AND DISCUSSIONS 25
4.1 Overview 25
4.2 Characterisation of AMD 25
4.3 Characterisation of tobacco wastes 26
4.4 Tobacco waste metal adsorption capabilities 27
4.4.1 Adsorbent loading rate effects 27
4.4.2 Adsorption isotherms modelling 29

4.4.3 Adsorption kinetics modelling 31
4.5 Tobacco waste in SRB mediated AMD bioremediation 34
4.5.1 Metal removal efficiencies 34
4.5.2 Sulfate reduction in biological AMD treatment 37
4.5.3 pH studies 38
4.5.4 The COD/SO_4 ratios during remediation 39
4.6 Physical observations 40
CHAPTER 5: CONCLUSIONS AND RECOMMENDATIONS 42
5.1 Overview 42
5.2 Conclusions 42
5.3 Recommendations 43
REFERENCES 45
APPENDICES 51
A1: Synthetic AMD Formulation 51
A2: Batch adsorption data at different adsorbent dosages (For Isotherms) and 14 hours runtime 52
A3: Adsorption data for adsorbent dosage of 80 g/L (For kinetics) in 14 hours runtime 53
A4: Metal ion concentrations during passive bioremediation 55
A5: Sulfate ion concentrations in AMD during bioremediation 58
A6: Changes in pH AMD passive bioremediation 59
A7: Changes in the COD of AMD during biotreatment 60

List of Figures

Figure 1: Effects of AMD in nature (a) Old metalliferous mine AMD from South Africa (Akcil & Koldas, 2006) (b) River suspected to be AMD contaminated by nearby mine activities in Dobsonvile, South Africa..... 6

Figure 2: Abiotic and biological techniques in AMD management 9

Figure 3: Experimental set up at University of Witwatersrand laboratories..... 200

Figure 4: Overall metal ion removals in AMD during adsorption (**a**) Synthetic (**b**) Industrial AMD 288

Figure 5: Adsorption isotherms for (a) Fe (b) Ni (c) Cu and (d) Zn on tobacco waste 311

Figure 6: Adsorption kinetics for (a) Fe (5) and (b) Fe (4) (c) Ni (d) Cu (e) Zn on tobacco waste 333

Figure 7(a-e): Metal concentration in aqueous media during bioremediation at 80 g/L of tobacco waste loading. The vertical error bars are SD of triplicate sample values. (a) is for Fe with initial concentration of 500 mg/L while (b) is for initial concentration of 420 mg/L. 366

Figure 8: Sulfate on concentration during biotreatment of (a) synthetic AMD and (b) industrial AMD. The vertical error bars are SD of triplicate sample values. 388

Figure 9: Variation of pH during bioremediation of (a) synthetic AMD (b) industrial AMD 3939

Figure 10: Ratios for COD/SO_4 concentration during bioremediation…….……40

Figure 11: Photographic results of day 22 showing sulfides precipitation in reactors..... ……411

List of Tables

Table 1: Examples of SRB carbon sources historically studied 1212
Table 2: Formulation of the modified Postgate C medium 19
Table 3: Equations used in analysing adsorption data 23
Table 4: Composition of AMD 25
Table 5: Composition of tobacco waste used in this study 26
Table 6: Adsorption isotherms model fitting parameters 30
Table 7: Kinetic modelling parameters for AMD metal adsorption onto tobacco waste 3232
Table 8: Exponential decay parameters for modelling metal ion concentration during bioremediation 35

List of Abbreviations, Symbols and Acronyms

AMD: Acid mine drainage

ARD: Acid rock drainage

C/N: Carbon to nitrogen ratios

COD: Chemical oxygen demand

CSIR: Council for Science and Industrial Research (South Africa)

DOC; Dissolved organic carbon

EAS: Easily available substrates

GDP: Gross domestic product

PBR: Permeable reactor barriers

pH: potential hydrogen

SAPS: Successive Alkalinity Producing Systems

SRB: Sulfate reducing bacteria

$q_{e:}$ solid phase equilibrium concentration of adsorbate on adsorbent (mg/g)

$q_{m:}$ maximum adsorption capacity of the adsorbent (mg/g)

q_t: adsorbate concentration on adsorbent after duration t during adsorption (mg/g)

C_e: equilibrium concentration of adsorbate in the solvent/liquid phase (mg/L)

K_L: Langmuir constant

R_L: separation factor

K_F: Freundlich constant

n: Freundlich heterogeneity parameter to be determined

K_S, β_S, α_S: Sips constants

k_1, k_2 and k_3: rate constants

k: exponential decay constant

CHAPTER 1: INTRODUCTION

1.1 Background

The phenomena of acid mine drainage (AMD), also known as acid rock drainage (ARD), takes place when sulfide-bearing material is exposed to oxygen and water, causing oxidation of the sulfide or sulfur to sulfate. The sulfate subsequently lowers the pH of the generated effluent, triggering the leaching out of metals in the ore or rocks (Skousen et al., 2017). Bacterial intervention can also facilitate the AMD process. The low pH of AMD effluent and presence of toxic heavy metals is detrimental to both flora and fauna. The AMD risks can be extended to human beings if AMD effluents find their way into natural water bodies that are used by humans for drinking, industrial processing and agriculture (Taylor et al., 2005). It is therefore prudent that AMD must be controlled or treated to avoid the aforesaid dangers. AMD management strategies are classified into biotic (biological) and abiotic systems (Akcil & Koldas, 2006; Johnson & Hallberg, 2005; Taylor et al., 2005). These two systems are further grouped into active and passive approaches. Active systems are more applicable to high volumes and at point of source AMD treatments especially for operating mines. These systems are generally more expensive, employing more energy and chemicals than passive ones (Johnson & Hallberg, 2005).

Passive treatment systems are systems that are designed to mimic the natural treatment processes found in natural ecosystems such as wetlands. These passive treatment systems provide a controlled environment in which natural chemical and biological reactions that help in the treatment of acid mine drainage can occur. Passive treatment systems are relatively new treatment technology that uses sulfate reducing bacteria or limestone or both to neutralize and precipitate metals. Passive systems are may be cheaper than active ones as they employ less energy and mild or no chemicals at all. These systems are may also be more stable in operation than active ones. Passive systems are readily applicable to old or abandoned mine sites. The appropriate selection of carbon sources used in passive AMD treatment can contribute to the environmental friendliness of the process. Because of these advantageous over active abiotic systems, there is increasing research focus and application of passive biotic systems (Simate & Ndlovu, 2014).

1.2 Sulfate reducing bacteria in AMD treatment

Passive biotic AMD treatment systems are driven by microorganisms called sulfate reducing bacteria (SRB). An example of such bacteria is *Desulfotomaculum nigrificans (D. nigrificans)* (Chockalingam & Subramanian, 2006). These bacteria facilitate AMD treatment by consuming the oxygen in the environment thereby creating anaerobic and alkaline conditions. These conditions favour reduction instead of oxidation. In this environment sulfates are reduced to sulfide when these SRBs are active and are supplied with a reliable organic carbon source for energy and growth under anaerobic conditions (Zhang & Wang, 2014).

1.3 Carbon sources for SRBs

Many studies have been conducted to identify suitable and cheaper organic carbon sources for the SRBs to perform their AMD waste management function (Burman et al.,2019; Muhammad et al., 2015; Ramla & Sheridan, 2015; Sánchez-Andrea et al., 2014; Zamzow et al., 2006). Different types of organic wastes for such materials have been studied and these include poultry manure, wood chip, sawdust, leaf, wine and cheese industry waste, rice straw and other organic materials. Many of these studies established that many organic matters are a good source of carbon for microbial remediation of AMD. It has also been proven that in general organic materials have good adsorption capacity for heavy metals (Zhang & Wang, 2014).

1.4 Problem statement

Locally, and therefore readily available, sources of organic carbon are required to sustainably implement passive biotic AMD treatment techniques under local conditions. Guidelines relating to organic wastes disposal into landfills has been recently amended to restrict dumping of high calorific value (>20 MJ/kg) materials in South Africa (Molewa, 2013). These wastes, such as tobacco processing waste, can be diverted from landfills and find potential application as organic carbon sources for bacteria in AMD treatment. Despite the numerous studies mentioned above and great potential in offering a dual solution to waste management problems by use of waste biomass in AMD treatment (Burman et al., 2018), no studies have been conducted using tobacco waste. There is therefore no publicly available knowledge regarding the use of tobacco waste as carbon source in AMD passive biotic treatment approach.

1.5 Hypothesis

In this study, it is postulated that tobacco waste which is a problematic waste in one industry can be a cheaper and sustainable source of the requisite organic carbon for sulfate reducing bacteria that drive the biotic passive treatment of AMD in the mining industry.

1.6 Validity of the study

Many studies have been conducted to identify suitable and cheaper organic carbon sources for the SRBs to perform their waste management function. The performance of different types of organic wastes in fulfilling this function has been reported for poultry manure, wood chips, sawdust, leaves, wine and cheese industry waste, rice straw and other organic materials. Many of these studies established that various organic materials are a good source of carbon for microbial remediation of AMD. It has also been proven that in general organic materials have good adsorption capacity for heavy metals (Zhang & Wang, 2014).

1.7 Research questions

The following are research questions for this study:

- Does tobacco waste have any sorption capacity for heavy metals in AMD?
- Can tobacco waste be used in conjunction with SRB towards a passive AMD treatment approach?

1.8 Aim and objectives

The overarching aim of this research is to investigate the potential use of tobacco waste as bio sorption material and carbon source (substrate) for sulfate reducing bacteria that play a role in the biotic passive treatment of acid mine drainage.

The specific objectives of the research are:

- To evaluate the heavy metals adsorption capability of tobacco waste.
- To evaluate SRB catalysed passive AMD treatment dependence on biomass (tobacco waste) concentration.

1.9 Outline of the dissertation

The present chapter gives an overview on what AMD is and the challenges associated with managing this phenomenon. The Chapter gives an introductory coverage about methods

employed to manage AMD and why the current methods prefer biotic passive systems approaches to active ones. It is further stated here that passive biotic systems require microorganisms to run and these sulfate reducing bacteria require a supply of an external carbon source to function properly. This narrows the discussion to the hypothesis and aims of this study whereby an organic matter waste stream from tobacco processing is being investigated for use as carbon source for SRB in AMD management. The research problem is stated followed by research questions and objectives. Chapter 2 comprise of a detailed literature survey that has informed the selection of this research topic and methodologies of the study. The experimental procedures are covered in Chapter 3. Results and discussions are furnished in Chapter 4. Lastly Chapter 5 presents the conclusions and recommendations arising from this study.

CHAPTER 2: LITERATURE REVIEW

2.1 Overview

This chapter provides a review of literature on AMD including different substrates used as carbon sources for the SRB mediated treatment of mine wastewater. Characteristics of tobacco processing wastes and their potential use in AMD treatment are also discussed.

2.2 Acid mine drainage formation

Mining and construction activities form the cornerstone of South Africa's economy with the mining sector creating employment for 2.3% of the country's working population (Maluleke, 2019) and consistently contributing around 7% towards the national GDP (Sorensen, 2011; Statistics South Africa Department, 2019). Mining also naturally creates a nucleus for many other economic activities. The South African construction industry contributes 4% to the national GDP and creates 8.4% employment in the country (Statistics South Africa Department, 2019). Despite all these benefits from mining and construction industries, a major environmental pollution associated with these two economic activities is acid mine drainage (AMD). Acid mine drainage also known as acid and metalliferous drainage (AMD) or acid rock drainage (ARD) refers to the process by which sulfides found in mining and construction waste are oxidised, leading to the subsequent release of pollutants and leaching of metals into mine waters (Akcil & Koldas, 2006; Matshusa-Masithi et al., 2009; Taylor et al., 2005). During subsurface mining, water flooding the mine is constantly pumped out to continue mining safely. When the mining life has come to an end, the pumping of water stops and the water floods the mines and eventually this acidic water flows into the natural environment (Johnson & Hallberg, 2005), as what happened in the 1992 case of Wheal Jane Mine where huge volumes of contaminants from that mine spilled into the environment (Colin, Paul G., Jeffery, & Margaret, 2005). Seepage from old mine tailing dams or ponds (Moncur & Ptacek, 2005), waste rock dumps and coal spoils (Tiwary, 2001) are also other sources of AMD. In Figure 1, images of typical effects of AMD are shown.

(a) **(b)**

Figure 1: Effects of AMD in nature (a) Old metalliferous mine AMD from South Africa (Akcil & Koldas, 2006) (b) River suspected to be AMD contaminated by nearby mine activities in Dobsonvile, South Africa (Mthethwa, 2014)

Taylor et al (2005) described the five commonly accepted chemical reactions that represent the chemistry of pyrite weathering (oxidation) to form AMD. These are restated as follows:

REACTION 1. The overall summary reaction – Weathering (oxidation) of pyrite

$4FeS_2 + 15O_2 + 14H_2O \rightarrow 4Fe(OH)_3 + 8H_2SO_4$ .....(1)

REACTION 2. Sulfur oxidation to sulfate with release of ferrous iron.

$2FeS_2 + 7O_2 + 2H_2O \rightarrow 2Fe^{2+} + 4{SO_4}^{2-} + 4H^+$.....(2)

REACTION 3. Conversion of Ferrous Iron to Ferric iron. *"rate determining step"*

$4Fe^{2+} + O_2 + 4H^+ \rightarrow 4Fe^{3+} + 2H_2O$.....(3)

REACTION 4. Hydrolysis of Iron

$Fe^{3+} + 3H_2O \rightarrow Fe(OH)_3 + 3H^+$.....(4)

REACTION 5. Oxidation of additional pyrite (or other metals) by ferric iron.

$MS_2 + 14\,Fe^{3+} + 8H_2O \rightarrow M^{2+} + 14Fe^{2+} + 2SO_4 + 16H^+$ .....(5)

Reaction 1 shows the oxidation of pyrite when it is exposed to atmospheric oxygen in the presence of water. Because the environment is oxidizing the sulfur or sulfide in the ore is

oxidized to sulfate with the subsequent release of ferrous iron as shown in reaction 2. This reaction produces two moles of acidity for every mole of pyrite oxidized.

In reaction 3, ferrous iron is converted to ferric iron by consuming the acidity. Certain bacteria increase the rate of oxidation from ferrous to ferric iron examples of which are *Acidithiobacillus ferrooxidans, Acidithiobacillus thiooxidans and Leptospirillum ferrooxidans* (Chockalingam & Subramanian, 2006). The bacteria participates in replenishing the ferric iron and protons that are consumed during the leach reactions (Hansford & Vargas, 2001). The rate for this reaction depends on pH whereby it is slow at low values (pH 2-3) with no bacteria present, and very fast at pH values near or above 5 (Gaikwad et al.,2010). It is therefore referred to as the 'rate determining step' in the overall acid-generation sequence (Simate & Ndlovu, 2014; Taylor et al., 2005).

Iron hydrolysis takes place in reaction 4 where the water molecule splits generating 3 moles of acidity and a precipitate of ferric hydroxide is formed when hydroxyl ions react with the ferrous iron. Hydrolysis results in the formation of metal hydroxide precipitates. This depends on pH (Skousen et al., 2017) with pH is above 3.5 promoting this reaction while below a pH of 3.5 little or no solid forms (Akcil & Koldas, 2006; Gaikwad, Sapkal, & Sapkal, 2010). Iron hydroxide precipitates only from water in equilibrium with atmospheric oxygen after it has been bacterially catalyzed or sufficiently aerated/oxidized to facilitate the conversion of soluble ferrous iron to soluble ferric iron. Other metals such as aluminum, manganese, arsenic, cadmium, copper, lead and zinc will also co-precipitate with iron to some degree.

Reaction 5 depicts the oxidation of additional pyrite or other metals by ferric iron. The ferric iron is generated in reaction 2 and 3. This is cyclic, self-propagation of the overall reaction and it takes place very rapidly and continues until either ferric iron or pyrite, and other metals are depleted. The oxidizing agent in this reaction is iron not oxygen.

As can be seen from reaction 5, the precipitation of Fe $(OH)_3$ is a key acid producing stage. Once sulfides have been oxidised to sulfate, it is extremely difficult to avoid oxidation of aqueous ferrous species to ferric species (reaction 2 & 3) and subsequent hydrolysis (reaction 4). With the

formation of ferric iron in the presence of fresh iron sulfide, further sulfide oxidation can be accelerated as represented in reaction 5.

2.3 AMD challenges

Economically the AMD significantly affect the mining or construction operations due to its corrosive effect on infrastructure, equipment and the limited recycling options of the discharge (Taylor et al., 2005). The biggest long-term economic impact comes at the time of closing down the mine in the form of the expense incurred on implementing effective closure options that take care of the AMD. In Johannesburg, South Africa, where heavily contaminated groundwater (as a result of oxidation of pyrite contained in the mine tailings dumps and has elevated concentrations of heavy metals) is near surface, it causes the upper 20 cm of soil profiles to be severely contaminated by heavy metals due to capillary rise and evaporation of the groundwater (Ochieng et al., 2010). Taylor et al. (2005) points out that AMD can cause revegetation and rehabilitation difficulties as it alters the soil chemistry leading to elemental excesses that are toxic to plants or elemental deficiencies that are key for plant growth.

2.4 Management of acid mine drainage

A number of strategies have been previously investigated and implemented at laboratory or commercial scale to manage AMD. The most popular commercial scale technique is the use of pH neutralizing agents to precipitate metal carbonates or hydroxides in an attempt to remove cations from the wastewaters (Kefeni et al., 2017). Membrane filtration systems and ion exchange resins have also been applied in removing cations from the AMD effluents (Agboola et al., 2017; Gaikwad et al., 2010; Mthethwa, 2014). Using the partially treated AMD as an agro-fertiliser has also been suggested and used successfully in South African olive plantations and other fruit trees as a measure to control transportation of AMD from point of generation to other sites (Akcil & Koldas, 2006). A detailed review of the various technologies and approaches to managing AMD revealed that most of the commercially available technologies are expensive and some are not very efficient (Anawar, 2015; Kefeni et al., 2017). The various interventions are classified as either biotic or abiotic. These remediation interventions are further sub classified into active and passive techniques. Biotic systems employ microorganisms to speed up the AMD treatment process while abiotic systems rely more on physical and chemical characteristics of the interventions. The use of sulfate reducing bacteria in treating AMD was discovered and

motivated for application as way back as 1968 (Tuttle et al., 1969). Active systems use lots of chemicals and energy while passive systems like wetlands use less energy and try to mimic naturally existing pollution abatement systems. It has been established that passive systems are easier and cheaper to implement than active ones (Anawar, 2015; Kefeni et al., 2017; Skousen et al., 2017) therefore passive biotic systems will be discussed further in this study. Figure 2 depicts the classification of most of the available AMD management options.

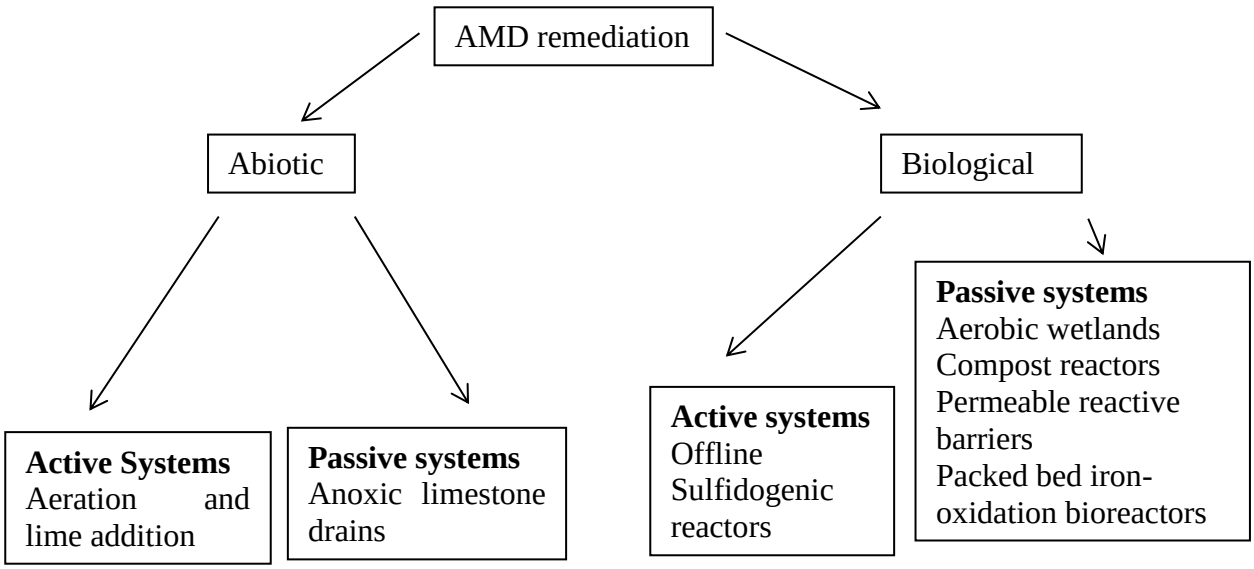

Figure 2: Abiotic and biological techniques in AMD management. Adapted from (Simate & Ndlovu, 2014)

2.4.1 Treating AMD through passive systems employing SRB

Biological passive treatment technologies employ sulfate reducing bacteria to facilitate AMD remediation. These bacteria use organic matter as source of energy to drive the sulfate reduction. Besides providing energy to the microorganisms, the carbon source materials also provide sorption platforms for metal cations and when sulfates are reduced alkalinity improvements trigger hydroxide or carbonate precipitation (Skousen et al., 2017; Zhang & Wang, 2014). The general reaction described here is as shown in reaction 6.

$$4SO_4^{2-} + 2CH_2O \rightarrow H_2S + 2HCO_3^- \quad \text{.....(6)}$$

CH_2O represents any simple carbon source.

Active sulfate reducing bioreactors are constructed to mimic the processes occurring within natural wetlands. The generation of alkalinity and precipitation of metals occurs in the same manner as in a natural wetland (Burman et al., 2018b). There are different types of passive sulfate reducing reactors such as composting or passive flow bioreactors which are completely sealed underground (Johnson & Hallberg, 2005); vertical flow systems in which AMD flows through the system vertically; Successive Alkalinity Producing Systems (SAPS) which have successive bioreactors in series (Kepler & McCleary, 1994); and Permeable Reactor Barriers (PRB) which are installed to intercept an underground AMD flow (Johnson & Hallberg, 2005a). SRBs in combination with carbonaceous materials achieve their task of pollution abatement by reversing the AMD formation reactions. In these systems, sulfate is reduced into sulfur and this increases the wastewater pH triggering the precipitation of metal hydroxides as well as carbonates. This set of conditions result in removal of metal cations from the wastewater. The carbonanceous material provides energy and is an electron donor to the microorganisms to sustain their metabolic processes. The carbon material can also act as an adsorbent. A pH range of 4-6 is ideal for microbial sulfate reduction processes (Simate & Ndlovu, 2014).

2.4.2 Carbon sources for SRB in treating AMD

Previous studies have been conducted with different organic wastes including grass and compost materials as a source of carbon and electron donor for microbial remediation of AMD (Chang et al., 2000; Chockalingam & Subramanian, 2006; Zagury et al.,2007; Greben et al., 2009; Lefticariu at al., 2015; Ramla & Sheridan, 2015; Burman et al.,2019). During anaerobic degradation, hydrolisation or decomposition of these organic wastes in the presence of sulfate occurs and soluble intermediate products including fatty acids are produced. This resembles the acid hydrolysis process employed to pre-treat lignocellulosic materials in commercial bio refineries (Reyes et al., 2016). Sulfate-reducing bacteria (SRB) use a wide range of substrates including branched and long chain fatty acids as electron donors and carbon sources, which oxidize incompletely to acetate or to CO_2 (Muhammad et al., 2015).

Studies investigating the use of cellulosic grass as a source of carbon for treatment of AMD revealed that the grass provides a suitable source of carbon and energy to SRBs as they reduce sulfate (Matshusa-Masithi et al., 2009; Burman et al.,2019). In the study by Matshusa-Masithi et

al. (2009) it was established that a COD/SO_4 ratio of greater than 0.67 mg/L provided sufficient organic matter to remove sulfate and once this ratio is less than 1 mg/L inhibition of the sulfidogenic process comes in with methanogenesis emerging as the favoured reaction under these conditions. The study further demonstrated that it is possible to use compost bacteria to degrade cellulose from grass cuttings that in turn provide carbon and energy source for the SRB bacteria in a biological reactor. In their study, Muhammad *et al*. (2015) established that mixed substrates of limestone, activated sludge, and spent mushroom compost were more effective in removing heavy metals and sulfate with great contribution of spent mushroom compost in the process than when substrates are used individually. In a similar study, Greben and co-workers (2009) performed bench top studies to determine the ability of grass combined with rumen fluid microorganisms to remediate AMD and they achieved sulfate removal efficiency of 78% with regular additions of grass cuttings to the system. Municipal wastewater has also been studied and its co-treatment with AMD gave impressive results with metal removals reaching as high as 99.8% while pH went up to 6.79 (Strosnider et al., 2011). Lefticariu and co-workers (2015) demonstrated in their study of limestone and organic matter bioreactors that the best type of organic matter for use in a bioreactor for SRB treatment of AMD would be the one with high herbaceous content.

The AMD wastewater is not only problematic due to its acidic nature but it also contains heavy metals which if not treated will still remain a significant pollutant in the SRB treatment of AMD effluent. Recent studies have also demonstrated the potential of treatment through heavy metal adsorption by agricultural waste by-products such as rice husks. Rice husks as a low cost adsorbent have been used to effectively remove heavy metals with concentrations of 20-60 mg/L in wastewater (Hegazi, 2013). More examples of biomasses previously used in AMD treatment are shown in Table 1. Tobacco waste products (stems and dust) being physico-chemically similar to some of the biomass discussed in this section by virtue of containing fibres, sugars, lignin *etc*., should have the potential to be used as low cost agricultural by-products for AMD treatment as proposed in this study. However, it is worth mentioning that high lignin content is not desirable as it naturally locks up nutrients from being accessed by microorganisms. Lignin itself is not biodegradable.

Table 1: Examples of SRB carbon sources historically studied

SRB carbon source options	**Advantages**	**Disadvantages**	**References**
Readily available nutrients (sugars, proteins, *etc*.)	Consumed easily by micro-organisms	Competition with human beings for food.	(Lindow & Borden, 2004, 2005)
Cellulosic wastes	Abundance. Cost effective relative to alkaline chemicals	Metal removal is slow	(Choudhary & Sheoran, 2012)
Chicken manure	Readily available at low cost as waste product	High sulfate reduction, sorption and hydroxide precipitation.	(Zhang & Wang, 2014)
Alcohols	Consumed more effectively by microorganisms than cellulosic materials	High cost of alcohol production.	(Buccambuso et al., 2007; Tsukamoto et al., 2004; Zamzow et al., 2006)
Lignin based	Very high cation removals above 95% for most AMD metals. Readily available in nature in huge quantities	Potential presence of phytochemicals in plant-based substrates may inhibit microbial performance. Substrates may require pretreatment like crushing to improve kinetics	(McCauley et al., 2008; Zagury et al., 2007) (Burman et al., 2018b; Burman et al., 2019)

2.4.3 Tobacco waste as carbon source for SRB in AMD treatment

As discussed in section 2.4.2 and shown in Table 1, different biomasses can be used to support SRB catalysed passive AMD treatment systems. Waste generated in tobacco processing consists of readily available nutrients like proteins and sugars (Leffingwell, 1999). It also contains cellulose, hemicellulose and lignin components which have different advantages in AMD treatment. This means the waste can potentially be usable in AMD treatment. If this happens, this will be a dual-purpose solution which solves challenges with tobacco waste disposal and at the same time addressing AMD treatment needs. In this study, the tobacco waste is used to treat AMD, another problematic waste from the mines. It is envisaged that AMD wastewater will consume the high COD inducing pollutants from the tobacco waste resulting in a safe effluent that can be disposed into the natural environment.

2.5 History and economic importance of tobacco processing

The word tobacco originated from the Spanish word ‘tabaco’. The plant is a native of the Americas and has been grown and used by the native Americans as far back as 1400–1000 BC. Tobacco plant belongs to the genus *Nicotiana* and of the *Solanaceae* (nightshade) family. There are more than 70 species of tobacco but the most common commercial crop is *N. tabacum*. The commercial species are, Virginia (flue cured), air cured (burley and cigar) and Oriental. The focus of this study shall be mainly on Virginia flue cured. Virginia tobacco grows in loam sandy soils and different climates but mostly in sunny climates. It grows up to 1.82m tall with large light-green leaves that are sticky with resin and tubular pink flowers with pale yellow centres. Tobacco leaves when dry, are used for smoking (cigarettes, cigar, and pipe tobacco) and consumed as snuff, chewing tobacco, dipping tobacco and snus (Lee, Hebert, Nonnemaker, & Kim, 2014)

Tobacco commands one of the most profitable industries in the world and contributes to huge positive fiscal economic impact in many countries (both developing and developed countries). Approximately 33 million people farm tobacco across the world and about half these people work in tobacco product manufacturing, distribution, and retailing. Another 10 million are employed in supplier industries providing materials and services to the tobacco industry for example, harvesting tools and cigarette papers, insurance coverage, transportation, shipping etc. Tobacco industry generates tens of billions of dollars annually in excise duty and taxation (Warner, 2000). About 90% of global tobacco farming takes place in India, China and Brazil (World Health Organisation, 2017). In some developing countries, such as Kenya, Zimbabwe and Malawi tobacco farming is the backbone of the economy.

2.5.1 Challenges from the tobacco industry

Although the tobacco industry contributes so much to the fiscal economies of different countries, its impact on human health and the environment (Ekpu & Brown, 2015) is so huge that the industry is experiencing serious pressure from anti-tobacco advocacy groups. Tobacco production figures are declining as more and more people quit smoking. According to the World Health Organisation, there are no safe levels of tobacco consumption and no safe investments in tobacco because tobacco kills and it saps national treasuries. The following statistics are reported on the World Health Organization website:

"……tobacco epidemic is one of the biggest public health threats the world has ever faced, killing more than 8 million people a year around the world. More than 7 million of those deaths are the result of direct tobacco use while around 1.2 million are the result of non-smokers being exposed to second-hand smoke".

Source: World Health Organisation (WHO, nd)

Besides health and economic impacts, tobacco also causes direct and indirect environmental impact. Environmental damage to the soil from tobacco growing, pesticides and fertilizer, and deforestation resulting from firewood use to cure tobacco; can impose high economic losses (World Health Organisation, 2017). Tobacco leaf processing and cigarette manufacturing also produces wastes and emissions that causes serious environmental pollution. Since this study is on the use of tobacco waste from leaf processing, much attention is given to the impact of tobacco leaf processing waste. This environmental waste from manufacturing activities has not been attracting a lot of research attention (Novotny et al., 2015). Tobacco manufacturing process produces immense amounts of waste. Globally, the industrial processing of tobacco leaves results in near 4% of waste with no commercial value at factories and of this, 95% is tobacco dust and 5% is tobacco stem (Tedesco et al., 2011). In Africa, most municipalities lack garbage removal resources and engineered landfill facilities. This results in solid waste (including tobacco waste) from households and industry ending up being dumped by the roadside, streams and riverbank creating health hazard and pollution of waterways (Mumba & Phiri, 2008). According to Mumba et al (2008), in Malawi, although the tobacco industries have a designated landfill for the disposal of tobacco process waste, the waste is dumped outside the landfill and by the roadside for community members to collect it and use it as manure for their fields. When it rains, this waste produces leachate, which is washed into nearby streams and rivers. Solid waste generated by tobacco industry poses an important environmental problem as some main components of tobacco waste are harmful and toxic and nicotine the principal alkaloid in tobacco is both toxic and harmful to health (Cosic et al., 2011). In most cases, the solid tobacco waste generated from the manufacturing plants end up in landfill or it is composted to produce a very high-quality fertilizer. However, these methods of disposal or treatment are associated with some potential environmental hazards, one of which is the production of nicotine-laden leachate. Leachate is generated by high moisture content wastes as it decomposes. Due to the high

solubility of nicotine in water, there is a serious risk that it can leach from wastes and may migrate to water bearing strata and end up contaminating groundwater aquifers and rivers and streams recharged from these aquifers (Cosic et al., 2011). In their studies on land disposal of tobacco processing residues, Tedesco et al. (2011) found out that tobacco waste contains high levels of ammonium nitrogen and potassium. Therefore, care is required when disposing tobacco waste on landfills as the leachate generated when the waste decomposes, can promote eutrophication if it flows into river systems.

With all the above mentioned environmental challenges posed by the disposal of tobacco waste via the conventional landfilling, it is important to find an alternative and environmentally sustainable way to dispose the waste where the pollutants (mainly nicotine, nutrients (N, K) are eliminated or reduced to acceptable ways.

2.6 Tobacco leaf chemistry and waste potential as SRB substrate

In general, a tobacco plant consists of those chemical substances that all plants have in common i.e. amino acids, sugars, and fats (Chemviews Magazine, 2014). More than 3000 chemicals identified and characterized in tobacco leaf, the major constituent is an alkaloid nicotine, which is a stimulant and powerful neurotoxin (Leffingwel, 1999). The tobacco leaf chemical composition depends on a number of aspects like genetics and the agricultural practices. It has been reported that high levels of nitrogen fertilizers infer high amino acids, protein, nicotine and nitrate levels in the leaf (Sheen, 1983). Oriental tobacco grown under limited supply of nitrogen nutrients and water, accumulation of acetate in the Krebs cycle and the subsequent biosynthesis of terpenoids via mevalonic acid as well as a higher production of carbohydrates, 'aromatic' acids and resins at the expense of nitrogen constituents has been witnessed (Leffingwell, 1976). Flue cured tobacco is intermediate in that the photochemistry during the plant's life cycle is balanced by a moderate supply of nitrogen which is depleted as the plant reaches maturity. Thus, flue cured tobacco and oriental tobacco contain significant amount of reducing sugars and lesser amount of α-amino nitrogen and protein. Reducing sugars are absent in air cured tobaccos.

Flue cured tobacco is harvested leaf by leaf as each ripe and the whole plant is harvest at once for burley tobacco. Changes associated with leaf maturity depending on the harvesting methods also affect the final leaf chemistry. The harvesting and curing processes change substantially the

chemical composition of the leaf. Enzymatic degradation of leaf constituents are halted by heat during flue curing in contrast, burley and oriental tobacco are not heated so that more extensive enzymatic changes occur. In flue-cured tobacco, enzymatic hydrolysis of starch to reducing sugars occurs at early stages of respiration in primed leaf, as the curing process continues enzymatic activity is arrested by the controlled desiccative dehydration during which eventually causes enzyme inactivation. In burley tobacco, starch accumulation is 25% during growth, this starch is depleted during the catabolic respiration of the plant while air curing leaving negligible sucrose and reducing sugars in the leaf (Leffingwell et al, 1999). Thus, flue-cured tobacco has more sugars than burley and burley tobacco have more protein and nitrates than flue-cured tobacco. Tobacco waste from flue-cured tobacco is therefore expected to perform better as carbon source for SRB treatment of AMD than burley.

A typical modern day tobacco leaf processing (Manickavasagan et al., 2007a, 2007b; Novotny et al., 2015) factory involves ten steps 1) Pre-conditioning 2) Blending 3) Picking 4) Conditioning 5) Feed Regulation 6) Threshing 7) Separating 8) Scrap Removal 9) Drying and 10) Packing. It is during steps 6 – 8 where tobacco dusts and stem waste is generated. The threshing process separates the lamina from the leaf stem. The lamina is the main product that is used for cigarette manufacturing. The stem and fine materials (tobacco dust) generated during the process becomes by-products and are discarded as tobacco waste. The leaf processing is a chemical free process with only steam and heat added during the conditioning stages. The industrial processing of tobacco leaves results in 4% of waste with no commercial value generated, of this 95% is tobacco dust and 5% is tobacco stem. The generation of dust and stem depends mainly on leaf quality and efficiency level of the industrial processing plant (Tedesco et al., 2011). Arising from the AMD formation chemical equation in section 2.2 and considering reaction 3 the ‘rate determining step’, it is important to note that the use of tobacco waste with alkalinity (pH of 5.1-6.5) (Tedesco et al., 2011) compared to that of AMD (pH of 2-3) should potentially increase the reaction rate of converting ferrous iron to ferric iron as this rate is several orders of magnitude faster at near neutral pH. Also critical for this bacterium aided reaction ‘rate-determining step’ is the energy needs (potentially provided by the sugar rich tobacco waste). Therefore, this reaction stage is the pith of this study wherein the use of tobacco waste as a carbon source, pH improver and adsorption sites provider in SRB catalyzed passive AMD treatment is proposed.

CHAPTER 3: EXPERIMENTAL METHODS

3.1 Overview

The section gives a breakdown of the experimental work executed to fulfil the objectives of this research. The materials used are described followed by the explanation of protocols used and a briefing on the laboratory experimental set up. The section concludes by stating how results were processed.

3.2 Materials and Chemicals

3.2.1 Chemicals

All chemicals used in this study were sourced from Sigma Aldrich, South Africa and were of analytical grade. Most of the chemicals were used in the formulation of synthetic AMD, the characterization of tobacco waste and the analysis of the treated AMD effluents.

3.2.2 Tobacco waste

The organic substrate (tobacco dust, 95% and stems, 5%) was collected from Limbe Leaf Tobacco Company in Malawi. This factory produces tobacco waste as a mixture of two types of tobacco (Flue cured tobacco and Barley). These two tobacco types have different physicochemical and biochemical characteristics. Flue cured tobacco has higher sugar content than the air cured barley tobacco. The flue cured wastes were preferred in this study because of the latter characteristic. Samples were collected as is from the factory while the factory was online and used within 3 days from the day of collection to avoid any material modification effects arising from compositing.

3.2.3 Synthetic AMD

Iron when associated with sulfur is the most popular metal in AMD wastewaters which after dissolution triggers the dissolution of other metals. In the synthetic AMD only iron and sulfate shall then be considered. The synthetic mine water solution was prepared according to literature (Ramla & Sheridan, 2015) with some modifications on the salt dosages whereby lower sulfate and iron levels were used in this study to mimic average typical industrial scale levels in South African AMD (Agbenyeku et al., 2016; Bologo et al., 2012; Henri et al., Wepener et al, 2014; Hobbs & Jude, 2007). Briefly, 12.4g of analytical grade ferrous sulfate salt ($FeSO_4.7H_2O$) was

dissolved in a beaker containing 5000 ml of distilled water. To this solution 10.9 g of 99% pure sulfuric acid was added and analytical grade caustic soda was added to adjust pH to 3. This formulation produced a synthetic AMD with a sulfate concentration of 3000 mg/L and a soluble iron concentration of 500 mg/L.

3.2.4 Industrial AMD

Acid mine drainage wastewater was collected from an AMD contaminated stream passing through a South African old mine dump located in Dobsonville, Johannesburg. In collecting the water sample, strict steps were followed to avoid contamination and ensure a representative sample is taken across the stream width. Sampling bottles were first rinsed with the site AMD immediately before use. After that, the sample was carefully collected making sure that sediments at the bottom of the stream were avoided.

3.2.5 Sulfate reducing bacteria and growth media.

The sulfate reducing bacterial culture used in the experiments was obtained from the existing stocks at the University of Witwatersrand, Johannesburg, School of Chemical & Metallurgical Engineering laboratory. This culture had been previously isolated from mine dumps exhibiting AMD in Gauteng. To 100 ml growth media, placed in a 150 ml Erlenmeyer flask, 5 ml of this culture (after it had been thawed from -80^{o}C storage to room temperature overnight) was added. The SRB was allowed to grow under anaerobic conditions at 30^{o}C in a shaker incubator for 14 days before its use in the assessment of tobacco waste (Zhang & Wang, 2014). Growth medium used for the SRB was modified Postgate C medium whose preparation in distilled water was as indicated in Table 2.

Table 2: Formulation of the modified Postgate C medium

Component	**Concentration (g/L)**
KH_2PO_4	0.5
NH_4Cl	1
Na_2SO_4	4.5
$CaCl_2.6H_2O$	0.06
$MgSO_4.7H_2O$	0.06
Sodium lactate	6
Yeast extract	1
$FeSO_4.7H_2O$	0.5
Sodium Citrate.$6H_2O$	0.3

3.3 Methods

3.3.1 Experimental set-up

Three sets of experiments were performed in triplicate as follows to fulfil different research objectives. For all the technical replicates, the reactors were set up in a shaker incubator as shown in Figure 3. Adsorbent/carbon source dosage and incubation time varied in different set ups (Set up 1, 2 and 3) to address different objectives as described below.

Set 1: To test for metal adsorption on tobacco waste and effect of adsorbent:AMD ratio

Four reactors containing different amounts (2-, 4-, 8- and 16 g respectively) of tobacco waste and equal amounts (100 ml) of the synthetic AMD were maintained at 30^{o}C temperature in a biochemical shaker incubator operated at 100 rpm for 15 hours. A fifth reactor containing synthetic AMD only and no tobacco waste was also included as a control. At 2-hour intervals, 2 ml solution of the reactor contents was filtered and measured for iron content using an Atomic Absorption Spectrometer (Make-Perkin Elmer PinAAcle 900H). This analysis was also performed at the end of the incubation period.

Set 2: Testing tobacco waste as carbon source for SRB and effect of substrate:AMD ratio

The same set up of five reactors as above was put together with the reactors taking (2-, 4-, 8- and 16 g respectively) tobacco waste in this order and same amounts of AMD (100 ml). Each reactor

was inoculated with 5 mL of SRB inoculum previously grown on the modified Postgate media (without lactate, yeast extract and sodium citrate, initial pH 5.0–5.5). Reactor 5 acting as the control received the inoculum only but no carbon source. All the reactors were incubated in a biochemical shaker incubator at 30^{o}C. Samples for measuring sulfate reduction levels, COD, pH changes and iron concentration as parameters for assessing bioremediation efficiency were taken at 4-day intervals over a 50-day period. The formation of black precipitate (FeS) and H_2S odour was also monitored.

Set 3 and 4: Replacing synthetic AMD with industrial AMD in biotreatment trial

The experimental set ups in 1 and 2 were repeated with industrial AMD effluent sourced from Johannesburg, South Africa being used instead of a synthetic AMD solution. Bioremediation towards more metal cations existing in the industrial AMD was evaluated.

Figure 3: Experimental set up at University of Witwatersrand laboratories

3.2.2 Tobacco waste characterisation

Substrate characterization followed the procedures described by Zhang et al. (2014). Upon collection from the factory site the moisture content, and organic matter content were determined using the standard gravimetric and weight difference APHA methods (APHA/AWWA/WEF, 2012). For other analysis, the tobacco samples were first dried at 75ºC and passed through a 2 mm sieve. From the 2 mm size class, 10 g were weighed, dissolved in 100ml of distilled water then agitated for 24 hours. The slurry was later centrifuged (my FUGE C1008-G -China), with the supernatant filtered (0,45µm filter) before analyses for dissolved organic carbon (DOC), bound nitrogen (N_b), pH and chemical oxygen demand (COD). DOC and N_b were determined by

a TOC analyzer (Vario TOC cube, Elementar) and dissolved (COD) was measured using the Merck COD kit with the Hatch spectrophotometer. Easily Available Substances EAS (soluble sugars, amino acids, protein and some other biodegradables portions) were assumed not to differ significantly with those found in literature like Leffingwell et al (1999) so the dextrose reducing sugars in this publication were taken to conservatively represent EAS for tobacco.

3.2.3 Metal cation measurements

Metal ions were measured in the AMD samples and the reacting batch mixtures. Slurry samples from each reactor were collected, centrifuged, filtered then acidified with one drop of nitric acid. The acidified clear solution was assayed for metals concentration at Civil and Environmental Engineering laboratories (Witwatersrand University, Johannesburg) using Atomic Absorption Spectroscopy (Perkin Elmer Atomic Absorption Spectrometer PinAAcle 900H) (Jawad et al., 2019). For quality control purposes, blanks and duplicates were run in parallel. The detection limit for the various metals was in the range 0.01 to 0.06 mg/L at 98% confidence level.

3.2.4 COD measurements

For dissolved COD measurements, the clear solution prepared in section 3.2.2 would be used with the Merck COD kit. Briefly, the clear sample (1 ml) is pipetted into a vial containing premeasured amounts of sulfuric acid and potassium dichromate. The vial is heated in a chamber at 150^{o}C for 2 hours in a standard digester block. After digestion and cooling down to room temperature, this vial is inserted into a spectrophotometer then the COD is read on the panel of a Hach Spectrophotometer. Most built-in Hach COD methods and calibrations can be used without the need for a new calibration.

3.2.5 pH measurements

Measuring pH for the reacting slurry was achieved by use of a hand help pH meter (FiveGoa F2). The pH meter probe is dipped in the reactor and then the pH reading displays on the instrument's panel after pressing read button. Buffer solutions were used to regularly calibrate the pH meter.

3.2.6 Sulfate concentration measurements

The technique used by Sheridan and Rimla (2015) was adopted to quantify sulfates in the reacting mixtures. Briefly, sulfate concentration was tested using a Shimadzu UV-Visible

Spectrometer (UV-1601). This involved adding barium chloride to the clarified solution of the reacting mixture which forms the insoluble barium sulfate. Sulfate ions were allowed to precipitate in an acid medium with barium chloride ($BaCl_2$) so as to form crystals of barium sulfate ($BaSO_4$) of uniform size. A photometer was used to measure light absorbance of the $BaSO_4$ suspension, and the SO_4^{2-} ion concentration was then determined using a previously developed standard calibration curve.

3.3 Results Analysis

Analytical results from the experimental set ups on each investigation highlighted in 3.3.1 were analyzed using Microsoft Excel. Mean values for the triplicate experiments were used in the final graphical plots and discussion of results with error bars expressed as standard deviations of the results also incorporated in graphical plots. Adsorption data for both synthetic and industrial AMD on tobacco waste were fitted to the common adsorption isotherms which are Langmuir, Freundlich and Sips. Although there are many isotherms that may describe adsorption, these three were identified to be popular and common in heterogeneous systems involving metal cations and solid adsorbents (Motsi et al., 2009). Non-linear regression modelling using MS excel based solver tool was used to fit the data. The best isotherm to describe the adsorption was selected on the basis of the highest coefficient of determination (R^2). The adsorption data was further used to model the kinetics of tobacco waste-metal cation adsorption over a period of 15 hours. Common kinetic models in adsorption which are the pseudo-first order and the pseudo-second order were investigated in this study (Simonin, 2016). The applicable equations for isotherm and kinetic modelling are shown in Table 3. Only, the 2-hr sample results at adsorbent dosage of 80 g/L were used in the kinetic modelling studies since this dosage had proved to be the optimal one among those tested for adsorption of metal cations in both synthetic and industrial AMD. This dosage was close to the technically optimal one in the sense that there was a significant increase in metal reduction as adsorbent dosage consistently rose from 20 through 40 to 80 g/L compared to the metal reduction increase achieved after this point. Increasing dosage from 80 to 160 g/L achieved minimal increase in metal removal per adsorbent across all metals as shown in Figures 4 and 6 of chapter 4.

Table 3: Equations used in analysing adsorption data

Expression name	Non-Linear version	Constants	Key attributes	References
Langmuir isotherm	$q_e = \frac{q_m K_L C_e}{1 + K_L C_e}$	K_L, q_m	Normally describes mono layer adsorption for dilute systems. Most suited isotherm for desulfurisation.	(Muzic et al., 2009)
Freundlich isotherm	$q_e = K_F C_e^{1/n}$	K_F, n	Non ideal irreversible and multilayer adsorption concepts.	(Proctor & Toro-Vazquez, 2009)
Sips isotherm	$q_e = \frac{K_s C_e^{\beta s}}{1 + \alpha_s C_e^{\beta s}}$	$K_s, \beta s, \alpha s$	Combines Freundlich and Langmuir behaviour to describe heterogeneous systems	(Sips, 1948)
PFO kinetics	$q_t = q_e(1 - e^{-k_1 t})$	k_1	Based on pseudo first order reaction equations.	(Azizian, 2004)
PSO kinetics	$q_t = \frac{q_e^2 k_2 t}{1 + k_2 q_e t}$	k_2	Successfully modelled metal removals from wastewater in previous studies	(Yuh Shan Ho, 2014)
Exponential decay	$A = A_0 e^{-kt}$	k	Models decreasing order values with time	(Westrich & Berner, 1984)

Symbols in this table are defined under symbols and acronyms page

For Langmuir adsorption, the separation factor (R_L) indicates whether adsorption is favorable or not (Hall et al., 1966). It is defined by Equation 1.

$$R_L = \frac{1}{1 + K_L C_0} \quad \text{.....(1)}$$

The process is irreversible where $R_L = 0$; favourable where $0 < R_L < 1$; unfavourable where $R_L > 1$ and becomes linear where $R_L = 1$;
For Freundlich isotherm, the adsorption is favourable when $n < 1$, unfavourable when $n > 1$ and becomes linear when $n = 1$.

From the general shape of the SRB mediated metal and sulfate removals in AMD, it was assumed that the metal removals followed an exponential decay as previously established

in other independent studies (Jorgensen et al., 2001; Westrich & Berner, 1984). Curve fitting with MS Excel solver was also performed to test this for all metals identified in the industrial AMD and bio-remediated at tobacco loading of 80 g/L.

CHAPTER 4: RESULTS AND DISCUSSIONS

4.1 Overview

This chapter reports and discusses the results obtained from the experimental study. The focus is on metal removal efficiencies from AMD by adsorption as well as by a combination of adsorption and SRB mediated passive treatment. Included in the discussion is sulfate reduction as well as changes in pH and COD during the batch AMD remediation.

4.2 Characterisation of AMD

The components of interest in both the synthetic and industrial AMD are reported in Table 3. For the synthetic AMD only the pH, iron and sulfate concentration were analyzed to check if the preparation had achieved targeted values. The industrial AMD contained more iron than other metals and the results were generally in close agreement with those reported from other AMD samples collected from this region of South Africa by other authors (Agboola et al., 2017). However, it cannot be overemphasized that AMD from different sources may differ significantly (Alegbe et al., 2019; Burman et al., 2018) in terms of composition, therefore site specific tests should be conducted first before implementing to full scale any laboratory based findings. Comparison of results and those from other studies as shown in Table 4 further confirms this point.

Table 4: Composition of AMD

Constituent	AMD Concentration in mg/L			
	(This study)		Other studies	
	Synthetic	Industrial	Synthetic (Chang et al., 2000)	Industrial (Choi & Lee, 2015)
Iron (Fe^{2+})	500	420.23	500	137.48
Nickel (Ni^{2+})	-	20.32	-	-
Copper (Cu^{2+})	-	38.21	50	22.78
Zinc (Zn^{2+})	-	5.73	100	19.77
Sulfate (SO_4^{2-})	3000	3318.23	2580	-
pH	3	2.7	6.8	2.41

4.3 Characterisation of tobacco wastes

The proximate and nutritional analysis results of tobacco waste are reported in Table 5. This waste is generally dry on an "as supplied" basis and hence its use in the metals adsorption or SRB mediated AMD treatment does not introduce unnecessary water volumes into the system. This property also makes tobacco waste handling and storage easier. The high percentage of organic matter (77%) in tobacco waste makes it a very good candidate for the intended use of SRB carbon source. It is the organic matter that provides the degradable carbon to the SRBs and hence enables these SRBs to function in facilitating the sulfate reduction (abatement). The C/N ratio of 35 in tobacco waste is conducive for most microorganisms to get enough energy from carbon and make internal cellular components from the nitrogen (Sitorus & Panjaitan, 2013). Carbon is well-known for its adsorption characteristic (Afkhami et al., 2007; Lalvani et al., 1998) and this also contributes to metal removal from the AMD effluent. Part of these organic components could however be locked in the crude fibre (7%) whose main component could be lignocellulosic. The AMD acidity is consumed during the hydrolysis of hemicelluloses to produce monomeric components (Burman et al., 2018b; Burman et al., 2019) and as this happens, the pH will increase.

Table 5: Composition of tobacco waste used in this study

Parameter	**Value**	**Units or basis**
Moisture	15.97	% of original wet mass
Organic matter	76.59	% of original wet mass
Bound nitrogen (N_b)	1.66	% of original wet mass
Protein (%)	4.29	% of original wet mass
Dissolved organic carbon (DOC)	57.73	% of original wet mass
Carbon to nitrogen (C/N) ratio	34.78	
*EAS (Reducing sugars)[1]	22.09	% of original wet mass
*Crude Fibre	7.08	% of original wet mass
*pH	5.45	pH meter

* Data extracted from (Leffingwell, 1999)

4.4 Tobacco waste metal adsorption capabilities

4.4.1 Adsorbent loading rate effects

When metal cations adsorption occurs onto the carbon source (adsorption surfaces) surfaces, the AMD effluent is depleted of these cations. Overall metal depletion reported as percentage metal removal was monitored (for both synthetic and industrial AMD set ups) through the measurement of the metal cations concentration remaining in solution after adsorption at different adsorbent loadings between 20 to 160 g/L. On the adsorbent loadings tested, it appeared that 80 g/L was close to the optimal one since there was continued significant gains in metal removal efficiencies between 20 and 80 g/L and very little thereafter. The overall metal recoveries from synthetic and industrial AMD after 15 hours incubation at different adsorbent loadings were plotted in Figure 4. The corresponding data is found on appendix A2.

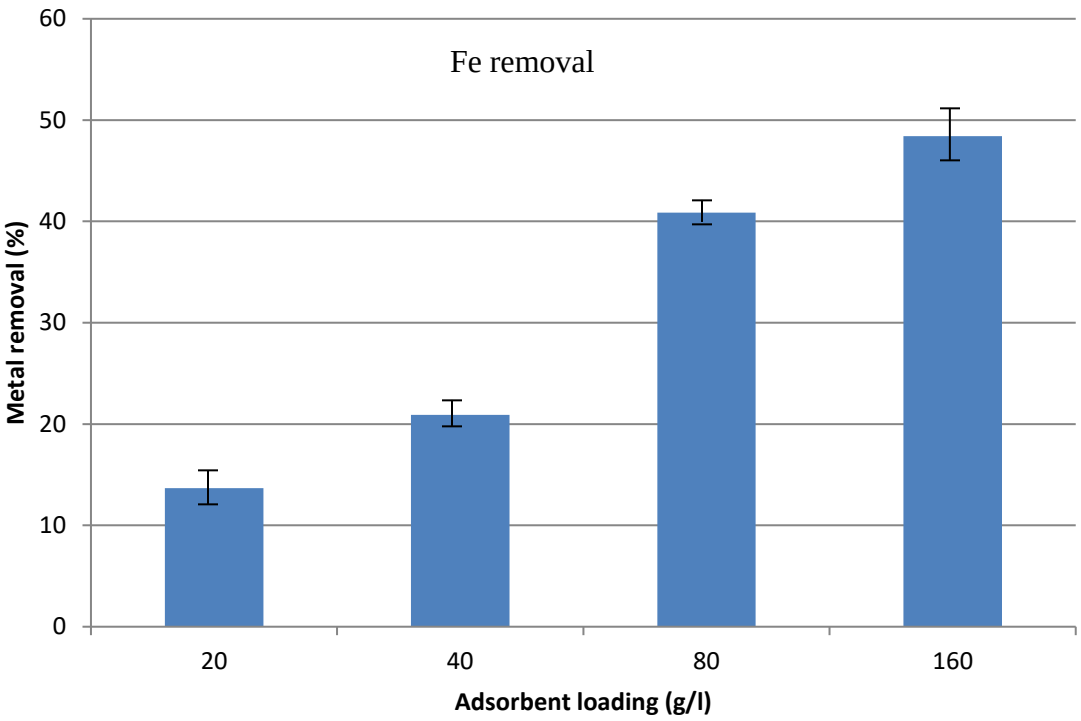

(a)

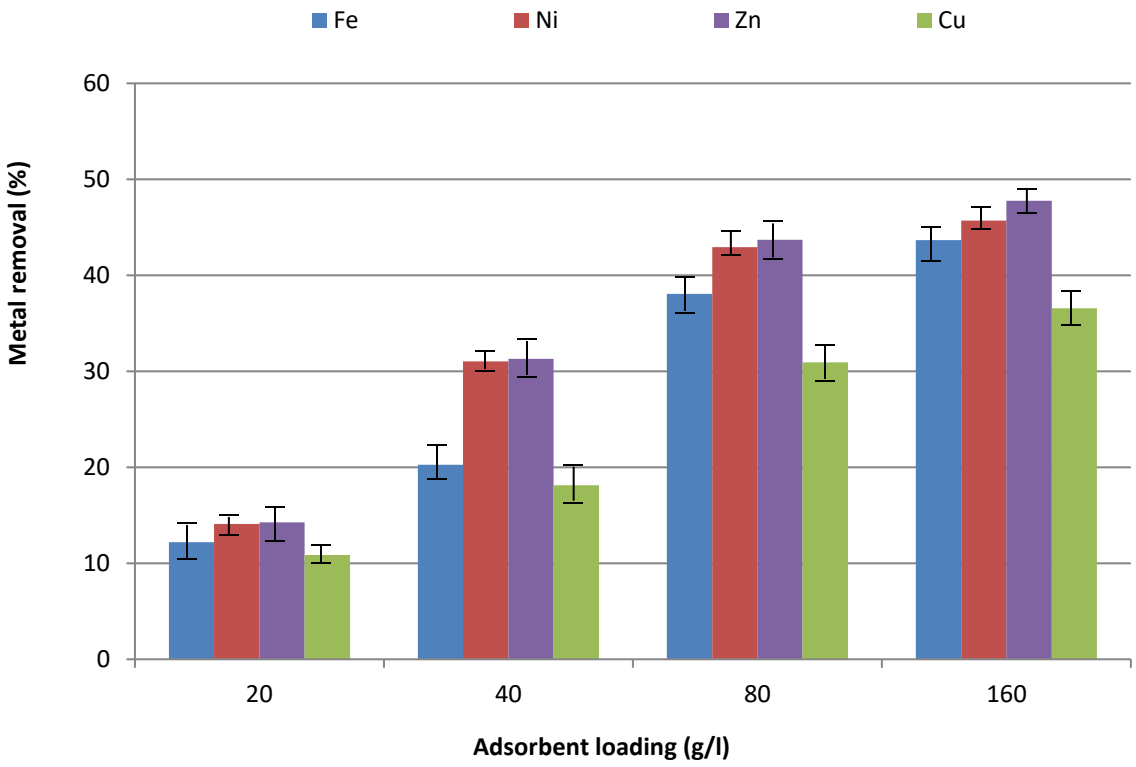

(b)

Figure 4: Overall metal ion removals in AMD during adsorption (**a**) Synthetic (**b**) Industrial AMD

During adsorption of iron in Figure 4a, there was a 50% increase in overall metal removal when the adsorbent loading increased by 100% from 20 g/L to 40 g/L. This increased overall metal removal with increase in adsorbent loading was even more pronounced at 80g/L where almost 100% increase was achieved after doubling the adsorbent loading from 40 g/L. In this case the overall metal removal jumped from 21% to 41%. However, when the adsorbent loading kept increasing the rate of increase in metal removal efficiency dwindled sharply. Doubling the dosage rate from 80-160 g/L improved the metal removal efficiency insignificantly from 41% metal recovery to 48%. The observed slowing down in metal removal per adsorbent loading may possibly be attributed to rheological challenges arising from increased solids concentration in the slurry which hinders the exposure of adsorption sites to the cations. The mixing efficiency could also have been affected at this high solids loading to effectively facilitate cation-to-surface

contact. During the adsorption of metals in industrial AMD (Figure 4b), increases in adsorbent loading also showed a corresponding increase in each metal removal although the numbers were not exactly matching those in Figure 4a. The same trends of increasing metal removals with increase in adsorbent loading were also reported by Hegazi (2013) in their AMD treatment experiments using rice husks and fly ash (Hegazi, 2013). In their study, they reported even higher overall metal removals because of the low initial metal concentrations in the AMD. However, the general trends are the same. The implication of a drop in the proportional rate of metal removal as adsorbent loadings go up, indicate that to operationalise tobacco waste use as metal adsorbent in AMD, an optimal dosage rate that balances out the cost of procuring the tobacco waste and process efficiency must be sought out.

In trials with industrial AMD, a reduction in overall efficiencies for iron cation at each loading was witnessed compared with synthetic AMD as depicted in Figure 4b. This may possibly be attributed to competition for active sites with other ions. The concentration of Ni is much lower. So even though the removal percentage is higher, the loading/removal of mg metal/g of tobacco waste is much higher for Fe. Therefore, the other metals do not have a significant effect on the removal of Fe compared with synthetic AMD where only Fe is existent in the solution. However, copper exhibits poorer adsorption characteristics than zinc and iron while zinc and iron adsorption performances are almost matching.

Using the industrial AMD for adsorption experiments, it was observed that the 80 g/L adsorbent loading was optimal for the different loadings tested. The overall metal removals for each metal over a 15-hour duration was plotted in Figure 4b, for each adsorbent dosage to glean more understanding on the metal recoveries (yields). It emerged that the previous observation noted in synthetic AMD treatment that more than 50% of the adsorption is completed in the first 2 hours was maintained. It was noted that zinc and iron adsorbs at almost similar yields while copper relatively struggles to adsorb as compared to the other metals in solution.

4.4.2 Adsorption isotherms modelling

The results of adsorption isotherms model fitting involving both synthetic and industrial AMD are reported in Table 6.

Table 6: Adsorption isotherms model fitting parameters

Adsorption isotherm	Metal/ Variable	Fe(5)*	Fe(4)#	Ni	Cu	Zn
Langmuir isotherm	q_m	1301.9	1209.0	317.6	20.8	107.0
	K_L	5.7E-06	5.8E-06	3E-5	2.8E-4	7.93E-05
	R_L	0.99	0.99	0.99	0.99	0.99
	R^2	0.95	0.78	0.78	0.85	0.77
Freundlich isotherm	K_F	0.0031	0.0010	0.0027	0.00023	0.0058
	n	0.87	0.75	0.71	0.51	0.79
	R^2	0.95	0.77	0.76	0.81	0.76
Sips isotherm	K_s	0.095	0.018	4E-06	5.33E-09	3E-06
	β	0.065	0.735	4.33	5.42	8.47
	α	-0.647	-0.006	2E-05	1.94E-08	6.98E-05
	R^2	0.96	0.75	0.87	0.91	0.96

*Fe(5) is for iron adsorption starting with initial concentration of 500 mg/L
#Fe(4) is for iron adsorption starting with initial concentration of 420 mg/L

Iron adsorption on tobacco waste showed that, starting with 2 different initial concentrations may affect the adsorption behaviour of the system. The adsorption model fitting showed higher coefficients of determination at higher initial iron concentration possibly because the higher concentration AMD was a purer sample which could not suffer from interaction effects from other metals as in the industrial sample. However, in both cases of higher and lower initial iron concentration, all three isotherm models studied, based on the R^2 values from Table 6, were equally suitable in modelling the dynamics of iron adsorption to tobacco waste. In all the other metals found in the industrial AMD, and the study conditions, the Sips isotherm fitted the data much better than the other two isotherms. The general goodness of fit was in the order Sips>Langmuir>Freundlich for copper, nickel and zinc ions. The Sips and Langmuir model's strength compared to the Freundlich in describing AMD metals adsorption to lignocellulosic substrates was also observed in other independent studies (Chockalingam & Subramanian, 2006; Ho et al., 2002; Singh et al., 2008). The Langmuir has also proved to supersede the Freundlich even in studies involving non-metals and inorganics adsorption (Ozacar, 2003). The best fitting performance demonstrated by the Sips in describing better the adsorption of many metals

compared to Langmuir and Freundlich isotherms is expected since the Sips model was developed to address the adsorbate concentration related weaknesses of both Freundlich and Langmuir models (Foo & Hameed, 2010). The isotherms that best fitted the experimental adsorption data for the various systems studied are plotted in Figure 5. The corresponding data is available in Appendix A2.

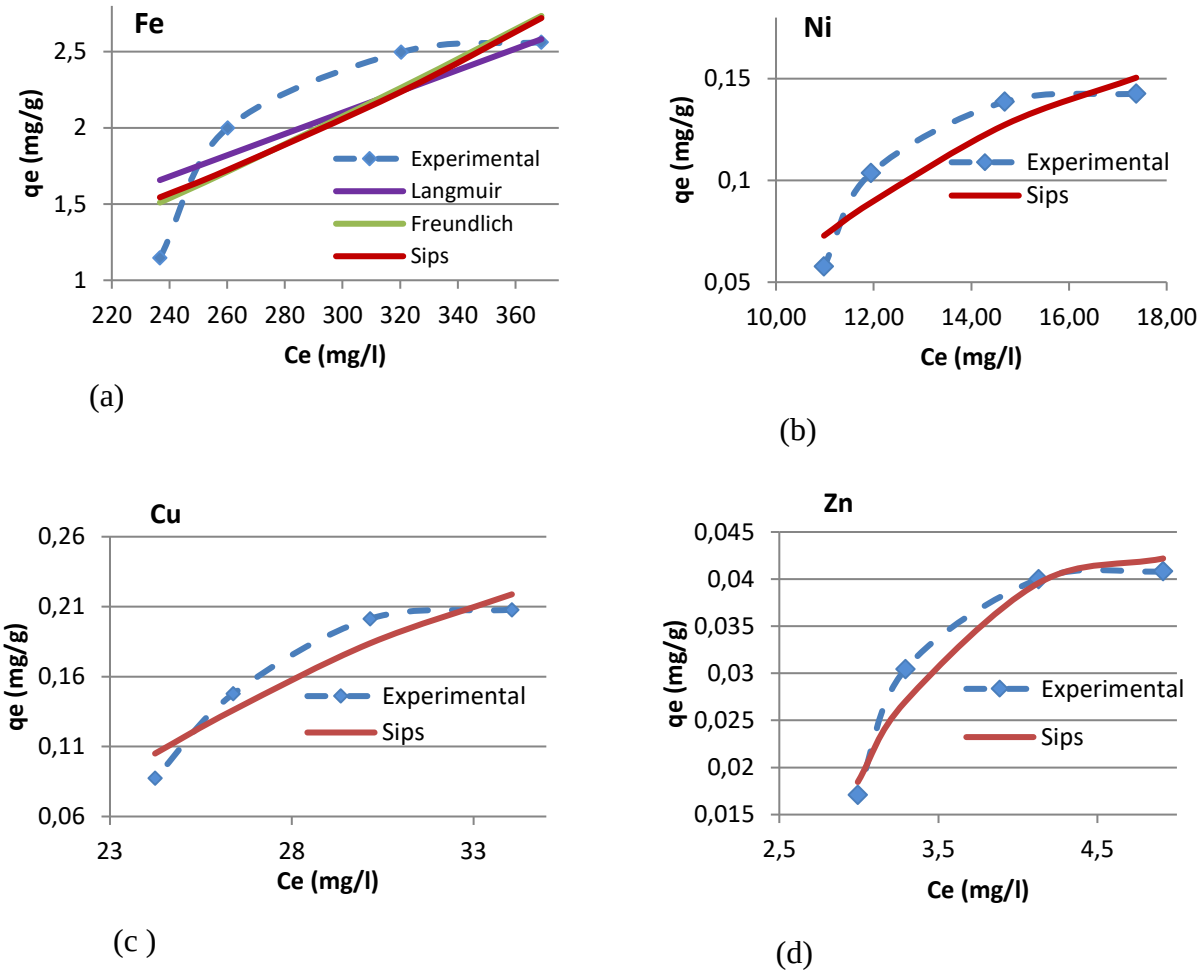

Figure 5: Adsorption isotherms for (a) Fe (b) Ni (c) Cu and (d) Zn on 80 g/L tobacco waste during 14 hours

4.4.3 Adsorption kinetics modelling

Experimental data showed that adsorption is a fast process in which more than 50% of the overall metals removal were achieved in the first 2 hours of the total 14-hour period. This is

significant as it will help the process if adsorption is coupled with biologically mediated remediation. During these first few hours metal removal by adsorption will reduce toxicity to microorganisms that will still be in the rapid growth phase and adaptation period. Meanwhile, the AMD acidity will also help in pretreating the carbon source through hydrolysis into monomeric easy to degrade metabolites. The adsorption data in this study was fitted to pseudo-first order and pseudo-second order models since these are the most popular kinetic models for adsorption. From the R^2 obtained it shows that the iron adsorption data fitted the pseudo first order model better than the second order model. The rest of the metals were better described by second order kinetics than the first order model. This general trend of second-order superiority to first-order models in most metal-adsorption systems was also observed by other researchers in independent studies (Ho et al., 1999; Moussout et al., 2018). The reason why iron was an exception to this trend could not be immediately established. The pseudo first-order and second-order constants as well as R^2 values are reported in Table 7 while the plots are displayed in Figure 6.

Table 7: Kinetic modelling parameters for AMD metal adsorption onto 80g/L tobacco waste

Kinetic Model	Metal/ Variable	Fe(5)*	Fe(4)#	Ni	Cu	Zn
Pseudo-first order	k_1	0.441	0.398	0.664	0.649	0.7
	R^2	0.95	0.99	0.987	0.983	0.96
Pseudo-second order	k_2	01.8E+14	0.505	19	10	34.8
	R^2	0.91	0.98	0.996	0.997	0.982

*Fe(5) is for iron adsorption starting with initial concentration of 500 mg/L
#Fe(4) is for iron adsorption starting with initial concentration of 420 mg/L

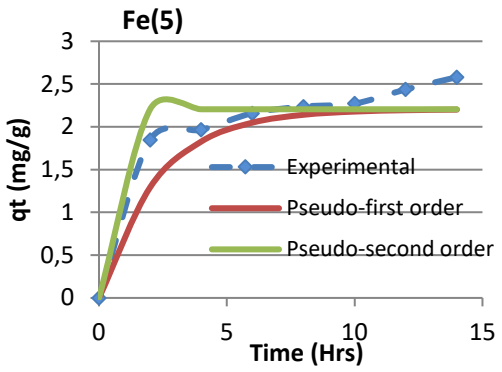

(a)

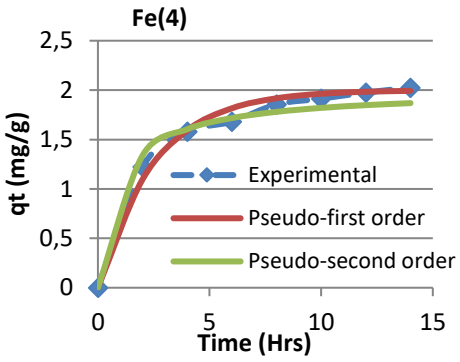

(b)

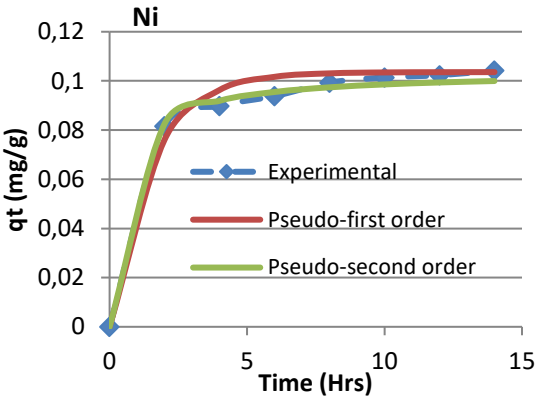

(c)

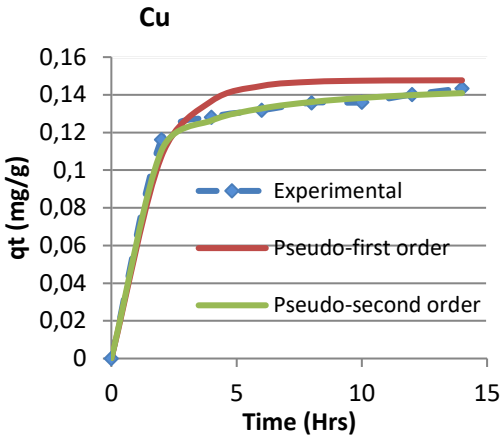

(d)

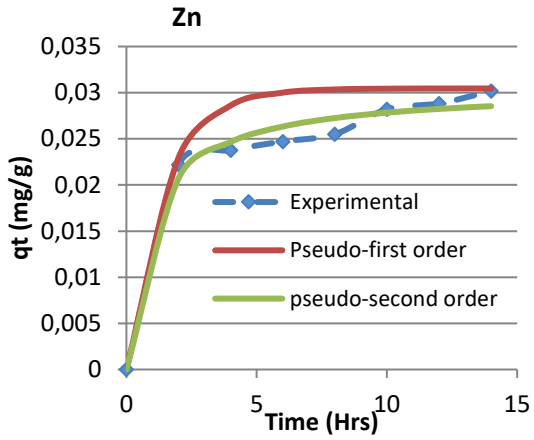

(e)

Figure 6: Adsorption kinetics for (a) Fe (5) and (b) Fe (4) (c) Ni (d) Cu (e) Zn on 80g/L tobacco waste

4.5 Tobacco waste in SRB mediated AMD bioremediation

These trials coupled microbiologically assisted AMD remediation with adsorption by adding tobacco waste in the AMD as the carbon source for the microbes. Besides the tobacco waste removing cations by adsorption, it also degrades by AMD induced hydrolysis to provide the nutrients required by SRB as they reduce sulfate into sulfide. The sulfides then precipitate out of the solution due to low solubility when compared to the sulfate. This precipitation removes both the metal cations and the sulfate which concurrently raises the AMD effluent pH. As higher pH manifests the environment becomes more conducive for SRBs performance and also induces further metal precipitations as hydroxides and carbonates. The same tobacco waste provides support material for the microorganisms as well.

4.5.1 Metal removal efficiencies

Carbon source (tobacco waste) dosage was maintained at the previously established optimal level of 80 g/L when bacteria were introduced into the remediation runs. In both the synthetic AMD and the industrial AMD trials, the overall metal removals went up to more than 70% when bacteria were introduced into the adsorption runs. The SRB trials however had to be extended to 50 days since bacterial remediation is generally slower than adsorption process in metal removal. The slowdown in metal removals accompanying SRBs inoculation may be attributed to conversion of some of the adsorbent material towards nutritional needs of the microorganisms. The reduced amount of available adsorbent for adsorption while the SRBs are still multiplying and growing is likely to impact on metal removal kinetics. As depicted in Figure 9, SRBs have high affinity for nickel than other metals. Here the nickel removal matched that of iron and zinc though from adsorption studies it had earlier been demonstrated that much of the iron and zinc is depleted through adsorption as compared to nickel. Interestingly copper continues to show poorer removals as previously observed in adsorption trials. While the reason for adsorption performance for copper may still be unclear the poor removals by SRBs could be attributed to the toxicity effects that has been identified to be associated with copper on many anaerobes (Lin & Chen, 1999; Yenigün et al., 1996; Yu & Fang, 2001). This copper toxicity affects the SRB's capacity to uptake this metal. The decrease in metal concentrations in the AMD solution as well as the sulfate concentrations were modelled by the exponential decay function (Singh et al., 2008) and using MS Excel curve fitting. Most of the experimental data fitted well to this model.

No further models were fitted. The exponential decay constants for the various metals are reported in Table 7 and the plots for experimental and curve fittings are shown in Figure 7.

Table 8: Exponential decay parameters for modelling metal ion concentration during bioremediation

Exponential Model	Metal/ Variable	Fe(5)	Fe(4)	Ni	Cu	Zn
Decay constants	C	21.5	9.0	0.5	9.8	0
	k_1	0.100	0.096	0.104	0.113	0.063
Coefficient of determination	R^2	0.97	0.99	0.99	0.97	0.95

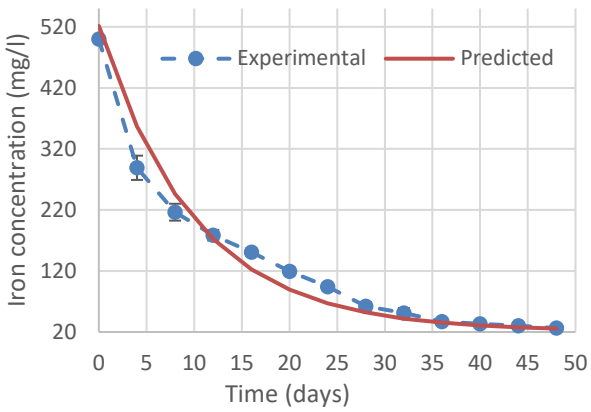

(a)

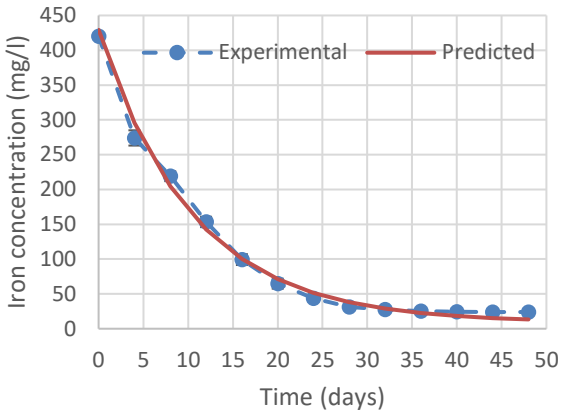

(b)

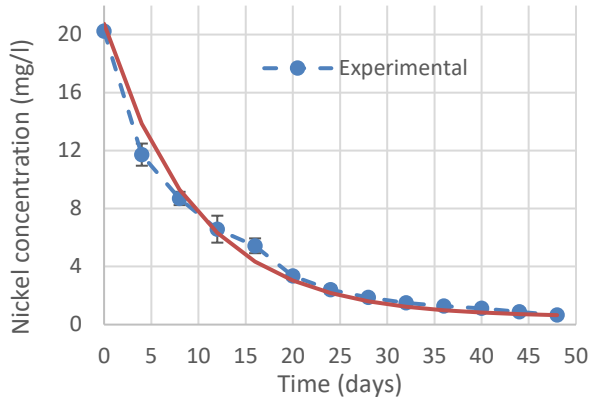

(c)

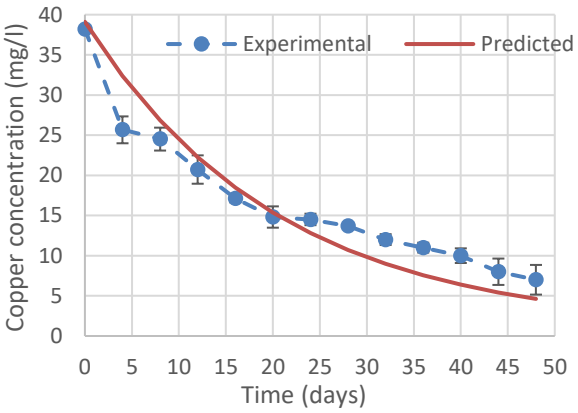

(d)

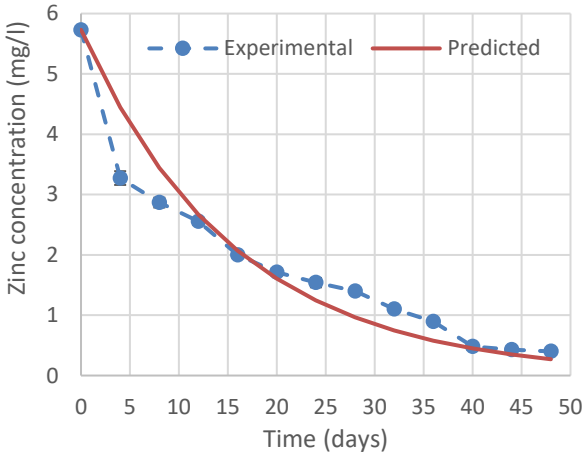

(e)

Figure 7(a-e): Metal concentration in aqueous media during bioremediation at 80 g/L of tobacco waste loading. The vertical error bars are SD of triplicate sample values. (a) is for Fe with initial concentration of 500 mg/L while (b) is for initial concentration of 420 mg/L.

4.5.2 Sulfate reduction in biological AMD treatment

The main purpose of introducing SRB bacteria into the AMD treatment is to reduce the sulfate levels in the effluent. In both cases of the synthetic and the industrial AMD as displayed in Figures 8a and b, the sulfate reduction was slow in the first 10 days. This sluggish reduction may possibly have been due to the microorganisms which were still adapting to the new environment and also required time to grow into an effective population. From around day 12 to day 20 there was rapid increase in sulfate removals starting at around 20% and shooting to as high as 60%. After day 20 the sulfate removal again slowed down till it plateaus from day 30. Day 36 to day 48 witnessed a gradual increase in sulfate concentration levels in the reactor indicating some dissolution of sulfides to sulfate. This was more pronounced in the industrial AMD and can be ascribed to the possibility of oxidative bacteria and competing bacteria existent in the industrial AMD that had gone dormant and only became active under those changing reactor conditions. The tobacco waste sulfate removal yields calculated will be 25 gSO_4/g.tobacco waste for the synthetic AMD and 29 gSO_4/g.tobacco waste. These results are quite encouraging being slightly above 20 times those of grass cutting obtained by Greben et al (2007) though these researchers were using an AMD of a different composition. The better performance of tobacco waste compared to grass cuttings may be attributed to improved surface areas in the finer dust of tobacco compared to coarser grass particles. Tobacco waste also comprise of higher easily available substrates (EAS) as shown in Table 5. Generally, grass is highly lignocellulosic (Burman et al., 2019; Greenhalf et al., 2012) and may require harsh conditions to unlock the easily degradable substrates. The decrease in sulfate levels of the aqueous AMD was fitted to exponential decay function as previously discussed and the plots shown on Figure 8 convey this message.

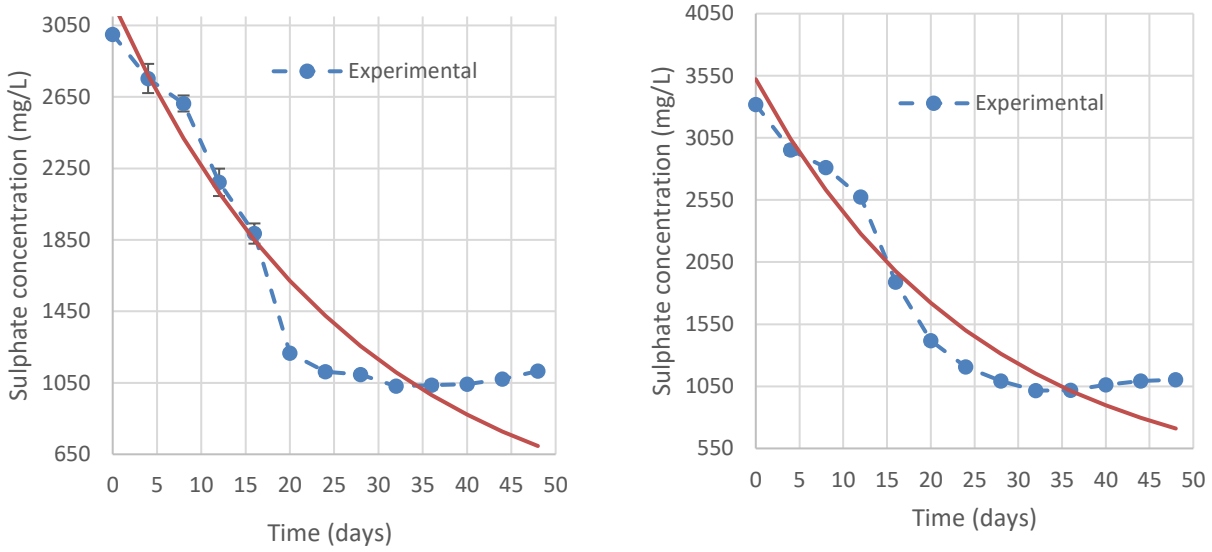

(a) (b)

Figure 8: Sulfate concentration during biotreatment of (a) synthetic AMD and (b) industrial AMD. The vertical error bars are SD of triplicate sample values.

4.5.3 pH studies

The removal of sulfate resulted in sulfide precipitation. This raised the effluent pH which triggers co-precipitation of metal carbonates and hydroxides. Since the sulfate removal was slow in the early days the pH followed that same trend also as depicted in Figure 9. Between day 10 and 35 the pH was increasing and only plateaued on approaching day 40. Overall, the pH of synthetic AMD improved by 2.05 units from 3.18 to 5.23. For the industrial AMD the pH increased by 2.41 units that is from an initial value of 2.75 to 5.16 after the incubation period. The tobacco waste demonstrated its potential to support SRBs during AMD treatment. Another possible outcome from tobacco waste usage is its potential contribution towards increasing AMD pH through both sulfate precipitation and waste consumption in hydrolysis of hemicelluloses to avail degradable organics to the bacteria.

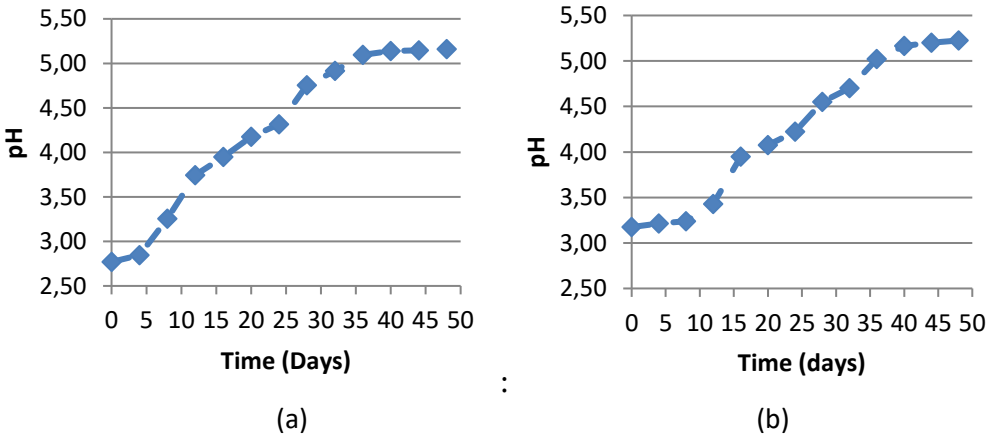

Figure 9: Variation of pH during bioremediation of (a) synthetic AMD (b) industrial AMD

4.5.4 The COD/SO_4 ratios during remediation

The ratios of COD to sulfate ion concentration during synthetic and industrial AMD bioremediation respectively are displayed in Figure 10. This ratio infers process stability and is expected to fluctuate between 0.55 and 0.67 (Greben, Tjatji, & Maree, 2004). Ratios higher than 0.67 indicate excess residual COD. This scenario may inhibit the microbial process through volatile fatty acid (VFA) inhibition. If a ratio is lower than 0.67, this signals excess sulfate concentration. This adversely affects the performance of the microorganisms in AMD remediation. In the trials conducted with tobacco waste it seems like the process is stable from beginning to the end if a dosage of 80 g/L is used in both synthetic and industrial AMD situations. The ratio ranged 0.56 to 0.93 throughout the incubation period as shown in the graphs. This also indicates that the degradable components from the tobacco waste are released gradually from the hemicellulose hydrolysis rather than all at once.

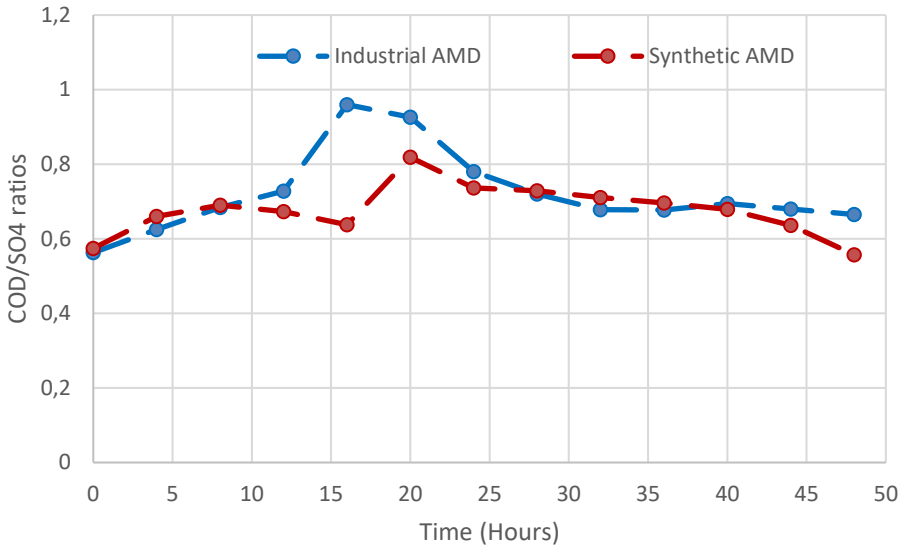

Figure 10: Ratios for COD/SO4 concentration during bioremediation

4.6 Physical observations

Photographs in Figure 11 show some of the observed physical changes that were taking place in reactors to confirm metal sulfide precipitations. In some reactors the 'rotten egg' smell of sulfur could be detected signalling the sulfate reduction to sulfur. Mixed bacterial (brown and whitish) growth and sulphide precipitations were observed in some batches with increasing intensity as days progressed from day 16 (7 December 2018). Other batches had no pungent smell and no growth especially the control batches. Also, some yellowish powder (sulfur) observed in some of the batches was associated was accompanied with the characteristic pungent smell of a rotten egg.

Figure 11: Photographic results for different days showing sulfides precipitation in reactors

CHAPTER 5: CONCLUSIONS AND RECOMMENDATIONS

5.1 Overview

This chapter summarizes the findings from the experiments conducted and also proposes future research directions.

5.2 Conclusions

Tobacco waste presents great potential for use as metal adsorbent in AMD treatment. When coupled with sulfate reducing bacterial the tobacco waste proved to be a good source for carbon to the bacteria. Using tobacco waste and SRB also partly resolved the AMD pH problem. Specific answers to the study's research questions are briefly provided below.

- **Does tobacco waste have any sorption capacity for heavy metals in AMD?**
  Tobacco waste proved that it can adsorb metal cations found in AMD. Under the experimental conditions of this study metals removal by batch adsorption ranged between 12-48% for the different metals depending on tobacco waste loading rate. However, there is room to improve this tobacco waste metal sorption capacity by manipulating different process parameters such as temperature, pH and hydraulic retention times. The adsorption of metals could be modelled by Langmuir isotherms for iron while the other metal cations fitted better to the Sips isotherm. The first order kinetics could also describe the iron adsorption well and the rest of the metals followed second order kinetics.

- **Can tobacco waste be used in conjunction with SRB towards a passive AMD treatment approach?**
  Tobacco waste can be used in SRB mediated AMD passive treatment since this substrate supported the growth of these microorganisms. The tobacco waste maintained a conducive COD/Sulfate ratio for SRBs throughout the experimental period. Evidence of passive AMD treatment came from the reduction in sulfate levels, detection of sulfur smell, the increased metal cations removal, the precipitation of sulfides in reactors as well as stable sulfate to COD ratio.

Although the removal efficiencies for most metal cations in AMD were relatively high in sulfate reducing bacterial assisted remediation in the presence of tobacco waste, copper seems to be poorly adsorbed and its uptake by SRBs was also low. Metal and sulfate ions concentrations in AMD during SRB biotreatment in the presence of tobacco waste can be deduced from exponential decay curve fitting models.

5.3 Recommendations

- Column tests are recommended in future to understand the long-term applicability of tobacco waste in AMD remediation. Possible toxicity and bacterial tolerance or adaptation to the potential toxics can only be deduced from long term continuous effluent feeding experiments.
- Working with co-substrates (Zagury et al., 2007) indicated that mixtures of substrates are better than single substrates so tobacco waste must be tried with other readily available biomasses in future. The selection of a co-substrate must be informed by a detailed characterisation (organic and inorganic elements) of both the main substrate (tobacco waste) and the candidate co-substrate.
- A cost benefit assessment must be performed to optimize adsorbent loading rates in the absence of significant mixing (a characteristic of passive remediation systems).
- Detailed adsorption studies with variations on temperature, metal initial concentrations and residence times are recommended in future studies to fully understand the adsorptive capacity and behaviour of tobacco substrate. This will also culminate into understanding the best applicable adsorption isotherms (Langmuir or Freundlich) which is critical in exploring the designs for commercial adsorbers in future. During these studies close monitoring of pH and sulphate levels, which was omitted in the current study would also be key to better understand the metal removal dynamics involved with tobacco waste.
- Safety (ecotoxicology studies) of treated effluent needs to be conducted to be sure that no hidden side effects may later on manifest if this effluent is disposed in public aquatic environments. No analysis of possible toxins was conducted during the bioremediation therefore future research must possibly explore this area on leachates. It is anyway encouraging that certain microorganisms like *Pseudomonas putida* have both AMD remediating and nicotine degrading characteristics and can be bioaugmented in these

passive AMD systems to exploit these benefits (Civilini et al.,1997; Chenbing et al., 2020).

- It may be necessary to couple passive biological AMD treatment with other cheaper methods to cater for recalcitrant components like copper in the effluent exiting these systems. Coupling passive bioremediation trials with safer processes such as phyto-remediation, filtration, fertigation, etc are recommended and needs further investigation. Other metals not tested in this study can also be included in future studies.
- Research to establish quantities of tobacco waste available for AMD adsorption purposes must be conducted. Inclusion of costs associated with transporting tobacco wastes from farming sites to mining sites should produce a good economics argument.

REFERENCES

Afkhami, A., Madrakian, T., Karimi, Z., & Amimi, A. (2007). Effect of treatment of carbon cloth with sodium hydroxide solution on its adsorption capacity for the adsorption of some cations. *Colloids and Surfaces A: Physicochemical Engineering Aspects*, *304*, 36–40.

Agbenyeku, E. O. E., Muzenda, E., & Msibi, M. I. (2016). Chemical alterations in three clayey soils from percolation and interaction with acid mine drainage (AMD). *South African Journal of Chemical Engineering*, *21*, 28–36. http://doi.org/10.1016/j.sajce.2016.04.003

Agboola, O., Mokrani, T., Sadiku, E. R., Kolesnikov, A., Olukunle, O. I., & Maree, J. P. (2017). Characterization of Two Nanofiltration Membranes for the Separation of Ions from Acid Mine Water. *Mine Water and the Environment*, *36*(3), 401–408.

Akcil, A., & Koldas, S. (2006). Acid Mine Drainage (AMD): causes, treatment and case studies. *Journal of Cleaner Production*, *14*, 1139–1145.

Alegbe, M. J., Ayanda, O. S., Ndungu, P., Nechaev, A., Fatoba, O. O., & Petrik, L. F. (2019). Physicochemical characteristics of acid mine drainage, simultaneous remediation and use as feedstock for value added products. *Journal of Environmental Chemical Engineering*, *7*(3).

Anawar, H. M. (2015). Sustainable rehabilitation of mining waste and acid mine drainage using geochemistry, mine type, mineralogy, texture, ore extraction and climate knowledge _ Elsevier Enhanced Reader.pdf. *Journal of Environmental Management*, *158*, 111–121.

APHA/AWWA/WEF. (2012). Standard methods for the examination of water and wastewater. *Standard Methods*. Washington D.C: American Public Health Association and American Waterworks Association and Water Environment Federation.

Azizian, S. (2004). Kinetic models of sorption: A theoretical analysis. *Journal of Colloid and Interface Science*, *276*(1), 47–52. http://doi.org/10.1016/j.jcis.2004.03.048

Bologo, V., Maree, J. P., & Carlsson, F. (2012). Application of magnesium hydroxide and barium hydroxide for the removal of metals and sulfate from mine water. *Water SA*, *38*(1), 23–28.

Buccambuso, E., Ruhs, A., Figueroa, L., Gusek, J. J., Holmes, W. M., & Reisman, D. (2007). Ethanol-fed or soli phase organic sulfate reducing bioreactors for the National tunnel drainage, Clear Creek / Central city superfund site? In R. I. Barnhisel (Ed.), *National Meeting of the American Society of Mining and Reclamation* (pp. 95–105). Lexington: ASMR.

Burman, N. W., Harding, K. G., & Sheridan, C. M. (2018). Use of Acidic Mine Drainage for the Pre-treatment of Lignocellulosic Biomass. In *International Water Association World Water Congress*.

Burman, N. W., Harding, K. G., Sheridan, C. M., Van Dyk, L. (2018a). Evaluation of a combined lignocellulosic/waste water biorefinery for simultaneous production of valuable biochemical products and the remediation of acid mine drainage. *Biofuels, Bioproducts and Biorefining*, *12*, 649–664. http://doi.org/10.1002/bbb

Burman, N. W., Sheridan, C. M., & Harding, K. G. (2019). Lignocellulosic bioethanol production from grasses pre-treated with acid mine drainage: Modeling and comparison of SHF and SSF. *Bioresource Technology Reports*, *7*(July), 100299.

Chang, I. S., Shin, P. K., & Kim, B. H. (2000). Biological treatment of acid mine drainage under sulfate-reducing conditions with solid waste materials as substrate. *Water Research*, *34*(4), 1269–1277.

Chenbing, A., Shanshan, H., Zhang, Y., Xiaoya, Z., Charles, A., Liyuan, C., Guanzhou, Q., Weimin, Z. (2020). Recovery of metals from acid mine drainage by bioelectrochemical system inoculated with a novel exoelectrogen, pseudomonas sp. E8. *Microorganisms, 8,* 2-16. http://doi.org/10.3390/microorganisms8010041

Chockalingam, E., & Subramanian, S. (2006). Studies on removal of metal ions and sulfate reduction using rice husk and Desulfotomaculum nigrificans with reference to remediation of acid mine drainage. *Chemosphere*, *62*(5), 699–708.

Choi, H., & Lee, S. (2015). Heavy metal removal from acid mine drainage by calcined eggshell and microalgae hybrid system. *Environmental Science and Pollution Research*, *3*, 13404–13411. http://doi.org/10.1007/s11356-015-4623-3

Choudhary, R. P., & Sheoran, A. S. (2012). Perfomance of single substrates in sulfate reducing bioreactor for the treatment of acid mine drainage. *Minerals Engineering*, *39*, 29–35.

Civilini, M., Domenis, C., Sebastianutto, N., De Bertoldi, M. (1997). Nicotine decontamination of tobacco agro-industrial waste and its degradation by micro-organisms. *Waste Management and Research, 15,* 349-358Colin, N., Paul G., W., Jeffery, H., & Margaret, N. (2005). The total water quality of River Carnon, west Cornwall, November 1992 to March 1994: the impacts of Wheal Jane discharges. *Science of the Total Environment*, *338*, 23–39.

Cosic, I., Marija, V., Nina, K., Dajana, K., & Felicita, B. (2011). Environmental Management. In *3rd International Symposium on Environmental Management: Towards Sustainable Technologies*.

Ekpu, V. U., & Brown, A. K. (2015). The Economic Impact of Smoking and of Reducing Smoking Prevalence : Review of Evidence. *Tobacco Use Insights*, *8*, 1–35.

Foo, K. Y., & Hameed, B. H. (2010). Insights into the modeling of adsorption isotherm systems. *Chemical Engineering Journal*, *156*(1), 2–10. http://doi.org/10.1016/j.cej.2009.09.013

Gaikwad, R. W., Sapkal, V. S., & Sapkal, R. S. (2010). Ion exchange system design for removal of heavy metals from acid mine drainage wastewater, *15*, 298–304.

Greben, H. A., Baloyi, J., Sigama, J., & Venter, S. N. (2009). Bioremediation of sulfate rich mine effluents using grass cuttings and rumen fluid microorganisms. *Journal of Geochemical Exploration*, *100*(2–3), 163–168.

Greben, H. A., Tjatji, M., & Maree, J. (2004). Biological sulfate reduction COD / SO4 ratios using propionate and acetate as the energy source for the biological sulfate removal in Acid Mine Drainage. In *IMWA Conference* (pp. 1–12). Newcastle Upon Tyne.

Greenhalf, C. E., Nowakowski, D. J., Bridgwater, A. V., Titiloye, J., Yates, N., Riche, A., & Shield, I. (2012). Thermochemical characterisation of straws and high yielding perennial grasses. *Industrial Crops and Products*, *36*(1), 449–459.

Hall, K. R., Eagleton, L. C., Acrivos, A., & Vermeulen, T. (1966). Pore- and solid-diffusion kinetics in fixed-bed adsorption under constant-pattern conditions. *Industrial and Engineering Chemistry Fundamentals*, *5*(2), 212–223. http://doi.org/10.1021/i160018a011

Hansford, G. S., & Vargas, T. (2001). Chemical and electrochemical basis of bioleaching processes. *Hydrometallurgy*, *59*, 135–145.

Hegazi, H. A. (2013). Removal of heavy metals from wastewater using agricultural and industrial wastes as adsorbents. *Housing and Building National Research Centre*, *9*, 276–282.

Henri, A. J., Wepener, V., Ferreira, M., Malherbe, W., & van Vuren, J. H. J. (2014). The effect of acid mine drainage on the hatching success of branchiopod egg banks from endorheic wetlands in South Africa. *Hydrobiologia*, *738*(1), 35–48. http://doi.org/10.1007/s10750-014-1913-6

Ho, Y. S. (2014). Using of "pseudo-second-order model" in adsorption. *Environmental Science and Pollution Research*, *21*(11), 7234–7235. http://doi.org/10.1007/s11356-013-2213-9

Ho, Y. S., Huang, C. T., & Huang, H. W. (2002). Equilibrium sorption isotherm for metal ions on tree fern. *Process Biochemistry*, *37*, 1421–1430.

Ho, Y. S., & McKay, G. (1999). Pseudo-second order model for sorption processes. *Process Biochemistry*, *34*(5), 451–465. http://doi.org/10.1016/S0032-9592(98)00112-5

Hobbs, P., & Jude, C. (2007). The Hydrogeology of the Krugersdorp Game Reserve Area and Implications for the Management of Mine Water Decant. In *Groundwater Division of the Geological Society of South Africa*. Bloemfontein.

Jawad, M., Arslan, M., Siddique, M., Ali, S., Tahseen, R., & Afzal, M. (2019). Potentialities of fl oating wetlands for the treatment of polluted water of. *Ecological Engineering*, *133*(May), 167–176.

John C. Leffingwell. (1999). Basic Chemical Constituents of Tobacco Leaf and Differences among Tobacco Types. In M. T. Nielson & D. D. Layten (Eds.), *Tobacco: Production, Chemistry and Technology* (pp. 266–284). Georgia, USA: Blackwell Science (Pub). Retrieved from http://www.leffingwell.com/download/tobacco_chemistry.pdf%5Cnhttp://www.leffingwell.com/leffrept.htm

Johnson, D. B., & Hallberg, K. B. (2005). Acid mine drainage remediation options: A review. *Science of the Total Environment*, *338*, 3–14. http://doi.org/10.1016/j.scitotenv.2004.09.002

Jorgensen, B. B., Weber, A., & Zopfi, J. (2001). SRBs in sea beds.pdf. *Deap-Sea Research 1*, *48*, 2097–2120.

Kefeni, K. K., Msagati, T. A. M., & Mamba, B. B. (2017). Acid mine drainage_ Prevention, treatment options, and resource recovery: A review. *Journal of Cleaner Production*, *151*, 475–493.

Kepler, D. A., & McCleary, E. C. (1994). Successive alkalinity -producing systems (SAPS) for the treatment of acidic mine drainage. In *International Land Reclamation and Mine Drainage Conference and the third International Conference on the abatement of Acidic Drainage* (pp. 195–204). Pittsburg: ASMR. http://doi.org/10.21000/JASMR94010195

Lalvani, S. ., Wiltowski, T., Hubner, A., Weston, A., & Mandich, N. (1998). Removal of hexavalent chromium and metal cations by selective and novel carbon adsorbent. *Carbon*, *36*(7–8), 1219–1226.

Lee, Y. O., Hebert, C. J., Nonnemaker, J. M., & Kim, A. E. (2014). Multiple tobacco product use among adults in the United States : Cigarettes , cigars , electronic cigarettes , hookah , smokeless tobacco , and snus. *Preventive Medicine*, *62*, 14–19.

Leffingwell, J. C. (1976). Recent advances in tobacco science: Leaf Composition and Physical Properties in Relation to Smoking Quality and Aroma. In *30th Tobacco Chemists Research Conference* (Vol. 2). Tennessee.

Lefticariu, L., Walters, E. R., Pugh, C. W., & Bender, K. S. (2015). Sulfate reducing bioreactor dependence on organic substrates for remediation of coal-generated acid mine drainage: Field experiments. *Applied Geochemistry*, *63*, 70–82.

Lin, C., & Chen, C. (1999). Effect of heavy metals on the methanogenic UASB granule. *Water Research*, *33*(2), 409–416.

Lindow, N. L., & Borden, R. C. (2004). Anaerobic bioremediation of acid mine drainage using EOS. In *America Society of Mining and Reclamation* (pp. 1192–1204). Lexington: ASMR.

Lindow, N. L., & Borden, R. C. (2005). Anaerobic Bioremediation of Acid Mine Drainage using Emulsified Soybean Oil. *Mine Water and the Environment*, *24*, 199–208.

Maluleke, R. (2019). *Quarterly Labour Force Survey Q2:2019*. *Quarterly Labour Force Survey* (Vol. PO211). Retrieved from www.statssa.gov.za

Manders, P., Hobbs, P., & Godfrey, L. (2009). *Acid Mine Drainage in South Africa*.

Manickavasagan, A., Gunasekaran, J. J., & Doraisamy, P. (2007a). Trends in Indian Flue Cured Virginia Tobacco (Nicotiana tobaccum) Processing : II . Threshing , Packing and Warehousing. *Research Journal of Agriculture and Biological Sciences*, *3*(6), 682–686.

Manickavasagan, A., Gunasekaran, J. J., & Doraisamy, P. (2007b). Trends in Indian Flue Cured Virginia Tobacco (Nocotiana tobaccum) processing II. Threshing, Packing and Warehousing. *Research Journal of Agriculture and Biological Sciences*, *3*(6), 676–681.

Matshusa-Masithi, M. P., Ogola, J. S., & Chimuka, L. (2009). Use of compost bacteria to degrade cellulose from grass cuttings in biological removal of sulfate from acid mine drainage. *Water SA*, *35*(1), 111–116.

McCauley, C. A., Sullivan, A. D. O., Weber, P. A., & Trumm, D. A. (2008). Perfomance of mesocosm-scale sulfate reducing bioreactors for treating acid mine drainage in New Zealand. In R. . Barnhisel (Ed.), *National Meeting of the American Society of Mining and Reclamation - New opportunities to apply our science* (pp. 662–698). Richmond, VA: ASMR.

Molewa, E. National Norms and standards for disposal of waste to landfill, Pub. L. No. 636 (2013). South Africa.

Moncur, M. C., & Ptacek, C. J. (2005). Release , transport and attenuation of metals from an old tailings impoundment. *Applied Geochemistry*, *20*, 639–659.

Motsi, T., Rowson, N. ., & Simmons, M. J. . (2009). Adsorption of heavy metals from acid mine drainage by natural zeolite.pdf. *International Journal of Mineral Processing*, *92*, 42–48.

Moussout, H., Ahlafi, H., Aazza, M., & Maghat, H. (2018). Critical of linear and nonlinear equations of pseudo-first order and pseudo-second order kinetic models. *Karbala International Journal of Modern Science*, *4*(2), 244–254.

http://doi.org/10.1016/j.kijoms.2018.04.001

Mthethwa, V. (2014). *Investigation of polyethersulphone (PES) hollow fiber membrane for the treatment of acid mine drainage*. University of Witswatersrand.

Muhammad, S. N., Kusin, F. M., Zahar, M. S. M., Halimoon, N., & Yusuf, F. M. (2015). Passive Treatment of Acid Mine Drainage Using Mixed Substrates: Batch Experiments. *Procedia Environmental Sciences*, *30*, 157–161. http://doi.org/10.1016/j.proenv.2015.10.028

Mumba, P. ., & Phiri, R. (2008). Environmental Impact Assessment of Tobacco Waste Disposal. *International Journal of Environmental Resources*, *2*(3), 225–230.

Novotny, T. E., Bialous, S. A., Burt, L., Curtis, C., Costa, V. L. da, Iqtda, S. U., … Espaignet, E. T. (2015). *The environmental and health impacts of tobacco agriculture, cigarette manufacture and consumption*.

Ochieng, G. M., Seanego, E. S., & Nkwonta, O. I. (2010). Impacts of mining on water resources in South Africa: A review. *Scientific Research and Essays*, *5*(22), 3351–3357.

Ozacar, M. (2003). Equilibrium and kinetic modelling of adsorption of Phosphorous on calcined alunite. *Adsorption*, *9*, 125–132.

Ramla, B., & Sheridan, C. (2015). The potential utilisation of indigenous South African grasses for acid mine drainage remediation. *Water SA*, *41*(2), 247–252.

Reyes, P., Márquez, N., Troncoso, E., Parra, C., Mendonça, R. T., & Rodríguez, J. (2016). Evaluation of combined dilute acid-kraft and steam explosion-kraft processes as pretreatment for Enzymatic hydrolysis of pinus radiata wood chips. *BioResources*, *11*(1), 612–625.

Sánchez-Andrea, I., Sanz, J. L., Bijmans, M. F. M., & Stams, A. J. M. (2014). Sulfate reduction at low pH to remediate acid mine drainage. *Journal of Hazardous Materials*, *269*(3), 98–109.

Sheen, S. J. (1983). Biomass and Chemical Composition of Tobacco Plants Under High Density Growth. *Beitrage Zur Tabakforschung International/ Contributions to Tobacco Research*, *12*(1), 35–42.

Simate, G. S., & Ndlovu, S. (2014). Acid mine drainage: Challenges and opportunities. *Journal of Environmental Chemical Engineering*, *2*(3), 1785–1803.

Simonin, J. (2016). On the comparison of pseudo-first order and pseudo-second order rate laws in the modeling of adsorption kinetics. *Chemical Engineering Journal*, *300*, 254–263.

Singh, A., Kumar, D., & J.P Gaur. (2008). Removal of Cu(II) and Pb(II) by Pithophora oedogonia:Sorption, desorption and repeated use of the biomass. *Journal of Harzadous Materials*, *152*, 1011–1019.

Sips, R. (1948). On the structure of a catalyst surface. *The Journal of Chemical Physics*, *16*(5), 490–495. http://doi.org/10.1063/1.1746922

Sitorus, B., & Panjaitan, S. D. (2013). Biogas recovery from anaerobic digestion process of mixed fruit -vegetable wastes. In *International Conference on Sustainable Energy Engineering and Application* (Vol. 32, pp. 176–182). Elsevier in Energy Procedia 32.

Skousen, J., Zipper, C. E., Rose, A., Ziemkiewicz, P. F., Nairn, R., Mcdonald, L. M., & Kleinmann, R. L. (2017). Review of Passive Systems for Acid Mine Drainage Treatment,

133–153.

Sorensen, P. (2011). Mining in South Africa: A mature industry? *International Journal of Environmental Studies*, *68*(5), 625–649.

Statistics South Africa Department. (2019). *Domestic Product Production*. Retrieved from http://www.statssa.gov.za/publications/P0441/GDP_2018_Q3_Media_presentation.pdf#page=14

Strosnider, W. H. J., Winfrey, B. K., & Nairn, R. W. (2011). Novel Passive Co-Treatment of Acid Mine Drainage and Municipal Wastewater. *Journal of Environmental Quality*, *40*(1), 206–213.

Taylor, J., Pape, S., & Murphy, N. (2005). A Summary of Passive and Active Treatment Technologies for Acid and Metalliferous Drainage (AMD). *Proceedings of the 5th Australian Workshop on Acid Drainage*, (29), 1–49.

Tedesco, M. J., Bortolon, L., Henrique, I. C., Clesio, G., & Marcio Henrique, L. (2011). Land disposal potential of tobacco processing residues. *Ciencia Rural, Santa Maria*, *41*(2), 236–241.

Tiwary, R. K. (2001). Environmental impact of coal mining on water regime and its management. *Water, Air and Soil Pollution*, *132*, 185–199.

Tsukamoto, T. K., Killion, H. A., & Miller, G. C. (2004). Column experiments for microbiological treatment of acid mine drainage : low-temperature , low-pH and matrix investigations, *38*, 1405–1418.

Tuttle, J. H., Dugan, P. R., & Randles, C. I. (1969). Microbial sulfate reduction and its potential utility as an acid mine water pollution abatement procedure. *Applied Microbiology*, *17*(2), 297–302.

Warner, K. E. (2000). The economics of tobacco : myths and realities. *Tobacco Control*, *9*, 78–89.

Westrich, J. T., & Berner, R. A. (1984). The role of sedimentary organic matter in bacterial sulfate reduction : The G model tested ’. *Limnology and Oceanography*, *29*(2), 236–249.

World Health Organisation. (2017). Tobacco and its environmental impact : an overview.

Yenigün, O., Kizilgün, F., & Yilmazer, G. (1996). Inhibition Effects of Zinc and Copper on Volatile Fatty Acid Production During Anaerobic Digestion. *Environmental Technology*, *17*, 1269–1274.

Yu, H. Q., & Fang, H. H. P. (2001). Inhibition on Acidogenesis of Dairy Wastewater by Zinc and Copper. *Environmental Technology*, *22*, 1459–1465.

Zagury, G. J., Neculita, C., & Bussiere, B. (2007). Passive treatment of acid mine drainage in bioreactors: Short review, applications, and research needs. In *Ottawa Geo2007* (pp. 1439–1446).

Zamzow, K. L., Tsukamoto, T. K., & Miller, G. C. (2006). Waste from Biodiesel Manufacturing as an Inexpensive Carbon Source for Bioreactors Treating Acid Mine Drainage, 163–170.

Zhang, M., & Wang, H. (2014). Organic wastes as carbon sources to promote sulfate reducing bacterial activity for biological remediation of acid mine drainage. *Minerals Engineering*, *69*, 81–90.

APPENDICES

A1: Synthetic AMD Formulation

Targets

Component	Concentration	
Fe	500	mg/L
SO_4^{2-}	3000	mg/L
pH	3	

Chemical proportions mixed

Component	g/L	mols
Fe	0.500	0.008929
$FeSO_4.7H_2O$ added	2.482	0.008929
SO_4^{2-} to come from w/$FeSO_4$	0.857	0.008929
SO_4^{2-} to come from w/H_2SO_4	2.140	0.022292
H_2SO_4 to be added	2.185	0.022292

The ferrous sulfate and sulphuric acid were added gradually into the beaker with gentle stirring then the prepared solution was topped up with water to the required volume in a conical flask.

A2: Batch adsorption data at different adsorbent dosages (For Isotherms) and 14 hours runtime

Iron (Fe^{2+}) in synthetic AMD during adsorption. Initial concentration is 500 mg/L

Adsorbent loading (g/L)	S1 (mg/L)	S2 (mg/L)	S3 (mg/L)	Ce (mg/L)	SD	Fe removed (mg)	Removal ratio (%)	q_e (mg/g)
20	431.48	431.45	431.97	431.63	0.238	68.37	14	3.418
40	395.48	394.98	395.71	395.39	0.305	104.61	21	2.615
80	335.05	320.29	315.41	323.58	8.349	176.42	35	2.205
160	258.01	257.89	257.78	257.89	0.094	242.11	48	1.513

Iron (Fe^{2+}) in industrial AMD. Initial concentration is 420.23 mg/L

Adsorbent loading (g/L)	S1 (mg/L)	S2 (mg/L)	S3 (mg/L)	Ce (mg/L)	SD	Fe removed (mg)	Removal ratio (%)	q_e (mg/g)
20	368.56	368.98	369.43	368.99	0.355	51.24	12	2.562
40	320.92	320.07	320.13	320.37	0.387	99.86	24	2.496
80	260.11	260.71	259.78	260.2	0.385	160.03	38	2.00
160	236.34	237.01	236.68	236.68	0.274	183.55	44	1.147

Nickel (Ni^{2+}) in industrial AMD. Initial concentration is 20.23mg/L

Adsorbent loading (g/L)	S1 (mg/L)	S2 (mg/L)	S3 (mg/L)	Ce (mg/L)	SD	Ni removed (mg)	Removal ratio (%)	q_e (mg/g)
20	16.23	17.98	17.92	17.38	0.81	2.85	14	0.143
40	14.66	14.77	14.62	14.68	0.06	5.55	27	0.139
80	11.94	11.97	11.92	11.94	0.02	8.29	41	0.104
160	10.96	11.01	10.98	10.98	0.02	9.25	46	0.058

Copper (Cu^{2+}) in industrial AMD. Initial copper concentration is 38.21 mg/L

Adsorbent loading (g/L)	S1 (mg/L)	S2 (mg/L)	S3 (mg/L)	Ce (mg/L)	SD	Cu removed (mg)	Removal ratio (%)	q_e (mg/g)
20	34.21	33.92	34.03	34.053	0.1195	4.157	11	0.208
40	30.17	30.16	30.13	30.153	0.017	8.057	21	0.201
80	26.34	26.17	26.67	26.393	0.2076	11.82	31	0.148
160	24.45	24.09	24.18	24.24	0.153	13.97	37	0.087

Zinc (Zn^{2+}) in industrial AMD. Initial zinc concentration is 5.73 mg/L

Adsorbent loading (g/L)	S1 (mg/L)	S2 (mg/L)	S3 (mg/L)	Ce (mg/L)	SD	Zn removed (mg)	Removal ratio (%)	q_e (mg/g)
20	4.91	4.96	4.87	4.91	0.037	0.816667	14	0.041
40	4.12	4.13	4.14	4.13	0.008	1.6	28	0.04
80	3.28	3.33	3.27	3.29	0.026	2.436667	43	0.030
160	2.98	3.01	2.99	2.99	0.012	2.736667	48	0.017

A3: Adsorption data for adsorbent dosage of 80 g/L (For kinetics) in 14 hours runtime

Fe^{2+} adsorption from synthetic AMD

Time (Hrs)	S1 (mg/L)	S2 (mg/L)	S3 (mg/L)	Ave (mg/L)	SD	Me removal (mg)	q_t (mg/g)
0	500	500	500	500	0	0	0
2	352.43	352.96	351.51	352.3	0.519	29.54	1.84625
4	343.45	342.05	342.79	342.7633	0.495	31.44733333	1.965458333
6	327.71	326.03	328.12	327.2867	0.783	34.54266667	2.158916667
8	320.08	320.92	321.97	320.99	0.67	35.802	2.237625
10	318.65	318.05	317.99	318.23	0.258	36.354	2.272125
12	305.07	305.74	304.33	305.0467	0.499	38.99066667	2.436916667
14	294.05	293.29	293.41	293.5833	0.289	41.28333333	2.580208333

Fe^{2+} adsorption in industrial AMD

Time (Hrs)	S1 (mg/L)	S2 (mg/L)	S3 (mg/L)	Ave (mg/L)	SD	Me removal (mg)	q_t (mg/g)
0	420.23	420.23	420.23	420.23	0	0	0
2	322.43	322.96	321.51	322.3	0.519	23.303905	1.224125
4	293.67	294.21	293.87	293.9167	0.193	30.05814276	1.578916667
6	285.54	286.06	285.63	285.7433	0.197	32.00310941	1.681083333
8	271.32	272.01	271.98	271.77	0.276	35.32827261	1.85575
10	267.37	266.97	267.09	267.1433	0.145	36.42925699	1.913583333
12	262.56	261.59	262.39	262.18	0.366	37.61035623	1.975625
14	258.11	258.01	258.78	258.3	0.296	38.53366014	2.024125

Ni^{2+} adsorption in industrial AMD

Time (Hrs)	S1 (mg/L)	S2 (mg/L)	S3 (mg/L)	Ave (mg/L)	SD	Me removal (mg)	q_t (mg/g)
0	20.23	20.23	20.23	20.23	0	0	0
2	13.65	13.75	13.72	13.70667	0.036	32.24583951	0.081541667
4	13.04	13.11	12.98	13.04333	0.046	35.52479815	0.089833333
6	12.67	12.69	12.81	12.72333	0.054	37.10660735	0.093833333
8	12.35	12.27	12.24	12.28667	0.04	39.26511781	0.099291667
10	12.15	12.11	12.09	12.11667	0.022	40.10545395	0.101416667
12	12.09	11.99	12.05	12.04333	0.036	40.46795189	0.102333333
14	11.85	11.94	11.88	11.89	0.032	41.22590213	0.10425

Copper adsorption in industrial AMD

Time (Hrs)	S1 (mg/L)	S2 (mg/L)	S3 (mg/L)	Ave (mg/L)	SD	Me removal (mg)	q_t (mg/g)
0	38.21	38.21	38.21	38.21	0	0	0
2	28.74	29.02	28.97	28.91	0.106	24.33917823	0.11625
4	28.05	27.89	27.96	27.96667	0.057	26.80799093	0.128041667
6	27.74	27.55	27.71	27.66667	0.072	27.59312571	0.131791667
8	27.37	27.33	27.35	27.35	0.014	28.42187909	0.13575
10	27.09	26.99	27.9	27.32667	0.353	28.48294513	0.136041667
12	26.96	27.05	26.99	27	0.032	29.33786967	0.140125
14	26.79	26.77	26.65	26.73667	0.054	30.02704353	0.143416667

Zinc adsorption in industrial AMD

Time (Hrs)	S1 (mg/L)	S2 (mg/L)	S3 (mg/L)	Ave (mg/L)	SD	Me removal (mg)	q_t (mg/g)
0	5.73	5.73	5.73	5.73	0	0	0
2	3.99	3.96	3.91	3.953333	0.029	31.00639907	0.022208333
4	3.85	3.81	3.83	3.83	0.014	33.15881326	0.02375
6	3.77	3.73	3.76	3.753333	0.015	34.49680047	0.024708333
8	3.69	3.67	3.71	3.69	0.014	35.60209424	0.0255
10	3.47	3.49	3.46	3.473333	0.011	39.38336242	0.028208333
12	3.41	3.44	3.42	3.423333	0.011	40.25596277	0.028833333
14	3.32	3.29	3.34	3.316667	0.018	42.11751018	0.030166667

A4: Metal ion concentrations during passive bioremediation

Iron in synthetic AMD treatment

Time (Hrs)	S1 (mg/L)	S2 (mg/L)	S3 (mg/L)	Ave (mg/L)	SD	Me removal (mg)
0	500.00	500.00	500.00	500	0.00	0
4	318.18	262.05	286.91	289	19.89	42
8	215.93	196.98	236.01	216	13.80	57
12	189.23	181.25	165.21	179	8.65	64
16	145.13	160.81	147.15	151	6.03	70
20	112.16	129.92	116.11	119	6.59	76
24	103.23	88.17	91.16	94	5.64	81
28	52.12	62.09	71.99	62	7.03	88
32	54.07	39.12	61.02	51	7.91	90
36	33.26	41.13	37.18	37	2.78	93
40	32.97	30.01	36.98	33	2.47	93
44	31.06	28.02	32.15	30	1.51	94
48	27.94	26.29	25.35	27	0.93	95

Iron in industrial AMD treatment

Time (Hrs)	S1 (mg/L)	S2 (mg/L)	S3 (mg/L)	Ave (mg/L)	SD	Me removal (mg)
0	420	420	420	420	0	0
4	259	273	290	274	11	35
8	209	229	219	219	7	48
12	142	156	162	153	7	64
16	110	88	100	99	8	76
20	53	72	69	65	7	85
24	47	40	43	44	2	90
28	31	27	36	31	3	93
32	30	26	28	28	1	93
36	25	26	25	25	0	94
40	24	24	24	24	0	94
44	24	24	24	24	0	94
48	24	24	24	24	0	94

Nickel in industrial AMD treatment

Time (Hrs)	S1 (mg/L)	S2 (mg/L)	S3 (mg/L)	Ave (mg/L)	SD	Me removal (mg)
0.00	20.23	20.23	20.23	20	0.00	0
4.00	11.76	10.62	12.78	12	0.76	42
8.00	7.96	9.18	8.95	9	0.46	57
12.00	6.95	5.12	7.67	7	0.93	67
16.00	6.21	4.78	5.31	5	0.51	73
20.00	3.75	3.08	3.24	3	0.25	83
24.00	2.03	2.78	2.42	2	0.27	88
28.00	1.76	2.09	1.77	2	0.13	91
32.00	1.45	1.67	1.35	1	0.12	93
36.00	1.13	1.42	1.25	1	0.10	94
40.00	1.03	1.24	1.11	1	0.07	94
44.00	0.87	0.85	0.89	1	0.01	96
48.00	0.65	0.68	0.63	1	0.02	97

Copper removal in industrial AMD treatment

Time (Hrs)	S1 (mg/L)	S2 (mg/L)	S3 (mg/L)	Ave (mg/L)	SD	Me removal (mg)
0	38.21	38.21	38.21	38	0.00	0.00
4	23.15	25.99	27.85	26	1.67	32.84
8	24.54	22.48	26.51	25	1.42	35.85
12	18.41	23.37	20.38	21	1.77	45.77
16	17.33	16.35	17.68	17	0.49	55.19
20	13.01	14.67	16.75	15	1.33	61.24
24	13.51	14.49	15.53	15	0.71	62.03
28	13.17	14.06	13.89	14	0.33	64.13
32	12.98	13.71	13.57	13	0.27	64.88
36	12.55	12.22	12.41	12	0.12	67.57
40	12.15	12.09	12.07	12	0.03	68.32
44	11.73	11.87	11.77	12	0.05	69.14
48	11.22	11.31	11.26	11	0.03	70.52

Zinc removal in industrial AMD treatment

Time (Hrs)	S1 (mg/L)	S2 (mg/L)	S3 (mg/L)	Ave (mg/L)	SD	Me removal (mg)
0	5.73	5.73	5.73	6	0.00	0.00
4	3.39	3.09	3.34	3	0.11	42.87
8	2.87	2.75	2.98	3	0.08	49.97
12	2.65	2.49	2.52	3	0.06	55.44
16	2.08	1.95	1.97	2	0.05	65.10
20	1.78	1.74	1.62	2	0.06	70.10
24	1.65	1.43	1.54	2	0.08	73.12
28	1.32	1.42	1.45	1	0.05	75.63
32	1.17	1.08	1.05	1	0.04	80.80
36	0.95	0.87	0.87	1	0.03	84.35
40	0.57	0.42	0.46	0	0.05	91.56
44	0.43	0.42	0.43	0	0.00	92.55
48	0.40	0.41	0.39	0	0.01	93.02

A5: Sulfate ion concentrations in AMD during bioremediation

Synthetic AMD sulfate concentrations during bioremediation

Time (Hrs)	S1 (mg/L)	S2 (mg/L)	Ave (mg/L)	SD	SO_4removal
0	3000.00	3000.00	3000	0.00	0
4	2853.11	2652.99	2753	81.70	8
8	2668.23	2558.17	2613	44.93	13
12	2078.01	2265.63	2172	76.60	28
16	1816.06	1954.63	1885	56.57	37
20	1236.45	1197.02	1217	16.10	59
24	1081.59	1142.05	1112	24.68	63
28	1071.10	1120.08	1096	20.00	63
32	1014.56	1047.06	1031	13.27	66
36	1067.08	1007.23	1037	24.43	65
40	1031.36	1051.52	1041	8.23	65
44	1056.12	1084.09	1070	11.42	64

Industrial AMD sulfate concentrations during bioremediation

Time (Hrs)	S1 (mg/L)	S2 (mg/L)	Ave (mg/L)	SD	SO_4removals
0	3318.18	3318.23	3318.205	0	0
4	2998.32	2905.43	2951.875	37.92	11.04068
8	2778.32	2842.37	2810.345	26.15	15.3059
12	2602.21	2543.99	2573.1	23.77	22.45565
16	1898.11	1878.03	1888.07	8.198	43.10009
20	1378.45	1454.18	1416.315	30.92	57.31715
24	1201.59	1212.25	1206.92	4.352	63.6276
28	1124.12	1060.81	1092.465	25.85	67.07688
32	1012.92	1018.06	1015.49	2.098	69.39664
36	1016.11	1018.21	1017.16	0.857	69.34631
40	1043.03	1081.99	1062.51	15.91	67.97962
44	1092.99	1095.09	1094.04	0.857	67.02941
48	1103.72	1104.01	1103.865	0.118	66.73332

A6: Changes in pH AMD passive bioremediation

Time	Synthetic AMD				Industrial AMD			
	S1	S2	Ave	SD	S1	S2	Ave	SD
0	3.19	3.16	3.18	0.01	2.76	2.74	2.75	0.01
4	3.17	3.22	3.20	0.03	2.85	2.84	2.85	0.005
8	3.25	3.23	3.24	0.01	3.27	3.24	3.26	0.015
12	3.44	3.42	3.43	0.01	3.74	3.75	3.75	0.005
16	3.92	3.98	3.95	0.03	3.92	3.98	3.95	0.03
20	4.08	4.07	4.08	0.00	4.18	4.17	4.18	0.005
24	4.22	4.23	4.23	0.01	4.32	4.31	4.32	0.005
28	4.55	4.58	4.57	0.02	4.75	4.76	4.76	0.005
32	4.65	4.71	4.68	0.03	4.91	4.92	4.92	0.005
36	5.01	5.03	5.02	0.01	5.09	5.10	5.10	0.005
40	5.16	5.17	5.17	0.00	5.13	5.15	5.14	0.01
44	5.19	5.21	5.20	0.01	5.14	5.15	5.15	0.005
48	5.23	5.22	5.23	0.01	5.18	5.14	5.16	0.02

A7: Changes in the COD of AMD during biotreatment

Time (Hrs)	Synthetic AMD				Industrial AMD COD			
	S1 (g/L)	S2 (g/L)	Ave (g/L)	SD	S1 (g/L)	S2 (g/L)	Ave (g/L)	SD
0	1723.03	1722.97	1723	0.03	1867.97	1868.02	1867.995	0.025
4	1817.43	1816.63	1817.03	0.326599	1845.03	1844.98	1845.005	0.020412
8	1804.12	1803.98	1804.05	0.057155	1923.11	1922.98	1923.045	0.053072
12	1460.78	1461.09	1460.935	0.126557	1872.69	1872.81	1872.75	0.04899
16	1203.06	1202.87	1202.965	0.077567	1812.27	1812.24	1812.255	0.012247
20	995.87	996.06	995.965	0.077567	1312.11	1312.09	1312.1	0.008165
24	818.86	819.03	818.945	0.069402	941.99	942.05	942.02	0.024495
28	798.79	798.57	798.68	0.089815	786.94	786.88	786.91	0.024495
32	732.45	732.64	732.545	0.077567	687.93	688.57	688.25	0.261279
36	722.35	722.32	722.335	0.012247	688.47	688.51	688.49	0.01633
40	706.68	706.72	706.7	0.01633	737.94	738.08	738.01	0.057155
44	680.37	680.32	680.345	0.020412	744.01	743.97	743.99	0.01633
48	621.75	621.83	621.79	0.03266	733.86	734.03	733.945	0.069402